Running Title: Nanosilver resistant *Proteus mirabilis*

Genome sequencing and analysis of the first spontaneous Nanosilver resistant bacterium *Proteus mirabilis* strain SCDR1

Amr T. M. Saeb [1*], Khalid A. Al-Rubeaan[1], Mohamed Abouelhoda [2, 3], Manojkumar Selvaraju [3, 4], and Hamsa T. Tayeb [2, 3]

1. Genetics and Biotechnology Department, Strategic Center for Diabetes Research, College of medicine, King Saud University, KSA.
2. Genetics Department, King Faisal Specialist Hospital and Research Center, Riyadh, KSA.
3. Saudi Human Genome Project, King Abdulaziz City for Science and Technology (KACST), Riyadh, KSA
4. Integrated Gulf Biosystems, Riyadh, KSA.
5. Department of Pathology & Laboratory Medicine, King Faisal Specialist Hospital and Research Center, Riyadh, KSA.
6. Department of Medicine, King Faisal Specialist Hospital and Research Center, Riyadh, KSA

***Corresponding Author:**

Amr T. M. Saeb, Ph.D.

Genetics and Biotechnology Department,

Strategic Center for Diabetes Research,

College of medicine, King Saud University, KSA.

Tel: +966-566263979

Fax: +966-11-4725682

Email: saeb.1@osu.edu

Abstract:

Background: *P. mirabilis* is a common uropathogenic bacterium that can cause major complications in patients with long-standing indwelling catheters or patients with urinary tract anomalies. In addition, *P. mirabilis* is a common cause of chronic osteomyelitis in Diabetic foot ulcer (DFU) patients. We isolated *P. mirabilis SCDR1* from a Diabetic ulcer patient. We examined *P. mirabilis SCDR1* levels of resistance against Nano-silver colloids, the commercial Nano-silver and silver containing bandages and commonly used antibiotics. We utilized next generation sequencing techniques (NGS), bioinformatics, phylogenetic analysis and pathogenomics in the characterization of the infectious pathogen. **Results:** *P. mirabilis SCDR1* is a multi-drug resistant isolate that also showed high levels of resistance against Nano-silver colloids, Nano-silver chitosan composite and the commercially available Nano-silver and silver bandages. The *P. mirabilis* -SCDR1 genome size is 3,815,621 bp. with G+C content of 38.44%. *P. mirabilis*-SCDR1 genome contains a total of 3,533 genes, 3,414 coding DNA sequence genes, 11, 10, 18 rRNAs (5S, 16S, and 23S), and 76 tRNAs. Our isolate contains all the required pathogenicity and virulence factors to establish a successful infection. *P. mirabilis* SCDR1 isolate is a potential virulent pathogen that despite its original isolation site, wound, it can establish kidney infection and its associated complications. *P. mirabilis SCDR1* contains several mechanisms for antibiotics and metals resistance including, biofilm formation, swarming mobility, efflux systems, and enzymatic detoxification**. Conclusion:** *P. mirabilis SCDR1* is the first reported spontaneous Nanosilver resistant bacterial strain. *P. mirabilis SCDR1* possesses several mechanisms that may lead to the observed Nanosilver resistance.

Keywords: *Proteus mirabilis*, multi-drug resistance, silver Nanoparticles, genome analysis, pathogenomics, biofilm formation, swarming mobility, resistome, Glutathione S-transferase, Copper/silver efflux system.

Background:

The production and utilization of nanosilver are one of the primary and still growing application in the field of nanotechnology. Nanosilver is used as the essential antimicrobial ingredient in both clinical and environmental technologies. (Chen and Schluesener 2008; Franci et al. 2015; Oyanedel-Craver and Smith 2008; Prabhu and Poulose 2012). Nanosilver is known to exert inhibitory and bactericidal effects activities against many Gram-positive, Gram-negative and fungal pathogens (Saeb et al. 2014). Latest studies suggest that the use of nanosilver-containing wound dressings prevent or reduce microbial growth in wounds and may improve the healing process (Velázquez-Velázquez et al. 2015). Moreover, antibacterial nanosilver-containing wound dressing gels may be important for patients that are at risk for non-healing of diabetic foot wounds and traumatic/surgical wounds (Lullove and Bernstein 2015). Increased usage of nanosilver in both medical and environmental products has generated concerns about the development of bacterial resistance against the antimicrobial ingredient. Bacterial resistance against metallic silver has been documented several bacterial strains such as *E. coli Enterobacter cloacae*, *Klebsiella pneumoniae* and *Salmonella typhimurium* (Hendry and Stewart 1979; McHugh et al. 1975). However, information about bacterial resistance against Nanosilver is in scarce. Only Gunawan et al., (2013) reported the occurrence of induced adaptation, of non-targeted environmental *Bacillus* species, to antimicrobial Nanosilver (Gunawan et al. 2013). In this study we are presenting of *Proteus mirabilis SCDR1* isolate, the first reported spontaneous Nanosilver resistant bacterial strain.

Proteus mirabilis is a motile gram-negative bacterium that is characterized by it swarming behavior (Jansen et al. 2003). Although it resides in human gut commensally, *P. mirabilis* is a common uropathogen that can cause major complications. In addition, *P. mirabilis* can cause respiratory and wound infections, bacteremia, and other infections (Mathur et al. 2005; Armbruster and Mobley 2012; Jacobsen et al. 2008). In fact, *P. mirabilis* is a common cause of chronic osteomyelitis in Diabetic foot ulcer (DFU) patients (Bronze and Cunha 2016). Generally, *P. mirabilis* is responsible for 90% of genus *Proteus* infections and can be considered as a community-acquired infection (Gonzalez and Bronze 2016). As a pathogen *P.*

mirabilis acquires many virulence determinants that enable it to establish successful infections. Alongside with mobility (flagellae), adherence, hemolysin, toxin production, Urease, Quorum sensing, iron acquisition systems, and proteins that function in immune evasion, are important virulence factors of *P. mirabilis* (Habibi et al. 2015; Baldo and Rocha 2014). A lot of information concerning antibiotic resistance are available for *P. mirabilis* (Horner et al. 2014; Miró et al. 2013; Hawser et al. 2014). *P. mirabilis* is intrinsically resistant to tetracyclines and polymyxins. Moreover, multidrug-resistant (MDR) *P. mirabilis* strains resistant resistance to β-lactams, aminoglycosides, fluoroquinolones, phenicols, streptothricin, tetracycline, and trimethoprim-sulfamethoxazole was reported (Chen et al. 2015). However, limited information about heavy metals, including silver, is available. In this study, we are presenting the first report and genome sequence of nanosilver resistant bacterium *P. mirabilis* strain SCDR1 isolated from diabetic foot ulcer (DFU) patient.

Materials and Methods:

Bacterial isolate:

Proteus mirabilis strain SCDR1 was isolated from a Diabetic ulcer patient in the Diabetic foot unit in the University Diabetes Center at King Saud University. Proper wound swab was obtained from the patient and was sent for further microbiological study and culture. Wounds needing debridement were debrided before swabbing the surface of the wound. Specimen was inoculated onto blood agar (BA; Oxoid, Basingstoke, UK) and MacConkey agar (Oxoid) and incubated at 37ºC for 24 - 48 h. The Vitek 2 system and its advanced expert system were used for microbial identification, antibiotic sensitivity testing, and interpretation of results. Manual disk diffusion and MIC method for AgNPs and antibiotic sensitivity testing were performed when required.

Preparation of colloidal and composite Nanosilver and Commercial products for antimicrobial activity testing:

Colloidal silver Nanoparticles were prepared, characterized and concentration determined as described by Saeb et al., 2014 (Saeb et al. 2014). Nanosilver chitosan composite preparations were done by chemical

reduction method as described by Latif et al., 2015 (Latif et al. 2015). Moreover, the following commercially silver and Nanosilver containing wound dressing bandages were also used for antimicrobial activity testing: Silvercel non-adherent antimicrobial alginate Dressing (Acelity L.P. Inc, San Antonio, Texas, USA), Sorbsan Silver dressing made of Calcium alginate with silver (Aspen Medical Europe Ltd., Leicestershire, UK), ColActive® Plus Ag (Covalon Technologies Ltd., Mississauga, Ontario, Canada), exsalt®SD7 wound dressing (Exciton Technologies, Edmonton, Alberta, Canada), Puracol Plus AG+ Collagen Dressings with Silver (Medline, Mundelein, Illinois, USA) and ACTISORB™ silver antimicrobial wound dressing 220 (Acelity L.P. Inc, San Antonio, Texas, USA).

Antimicrobial Susceptibility Test:

Antimicrobial activities were performed against the following strains: *Pseudomonas aeruginosa* ATCC 27853, *Staphylococcus aureus* ATCC 29213, *Proteus mirabilis* ATCC 29906, *Klebsiella pneumoniae* ATCC 700603, *E. coli* ATCC 25922 and *Enterobacter cloacae* ATCC 29212.

Disk diffusion antimicrobial susceptibility testing:

Disk diffusion antimicrobial susceptibility testing was performed as described by Matuschek et al. (Matuschek et al. 2014). The sterile discs were loaded with different concentrations (50-200 ppm) of colloidal silver nanoparticles solutions and the Nanosilver chitosan composite (composite concentration ranged between 0.1% and 0.01M to 3.2% and 0.16M from chitosan and Silver nitrate respectively) and then placed on Mueller–Hinton (MH) agar plates with bacterial lawns. Within 15 min of application of antimicrobial disks, the plates were inverted and incubated 37◦C for 16 hours. All experiments were done in an aseptic condition in laminar air flow cabinet. After incubation, inhibition zones were read at the point where no apparent growth is detected. The inhibition zone diameters were measured to the nearest millimeter. Similarly, 5mm desks from the commercially available bandages were prepared in an aseptic condition and tested for their antimicrobial activity as described before.

Minimum bactericidal (MBC), Minimal inhibitory concertation (MIC) and Biofilm formation tests:

MBC and MIC testing were performed as described by Holla et al., (Holla et al. 2012). Different volumes that contained a range of silver Nanoparticles (50-700 ppm) were delivered to 7.5 ml of Muller-Hinton

(MH) broth each inoculated with 0.2 ml of the bacterial suspensions. Within 15 min of application of silver nanoparticles, the tubes were incubated at 37◦C for 16 hours in a shaker incubator at 200 rpm. We included a positive control (tubes containing inoculum and nutrient media without silver nanoparticles) and a negative control (tubes containing silver nanoparticles and nutrient media without inoculum). Biofilm formation ability of *P. mirabilis* SCDR1 was tested as described before by Yassien and Khardori (Yassien and Khardori 2001).

Molecular Genomics analysis:

DNA purification and Sequencing:

Maxwell 16 automated DNA isolation machine was used for DNA isolation according to the instructions of the manufacturer. Isolated DNA was quantified using NanoDrop 2000c UV-Vis spectrophotometer. The Agilent 2100 Bioanalyzer system will be used for sizing, quantitation and quality control of DNA. The quality of subjected DNA sample was determined by loading a 150 mg of diluted DNA in 1% agarose E-gel (Invitrogen, Paisley, UK). We have conducted two sequencing runs using the Personal Genome Machine (PGM) sequencer from Life Technologies (Thermo Fischer) according to the instructions of the manufacture.

Bioinformatics analysis:

We have developed an analysis pipeline to identify the suggested pathogen and annotate it. First, the quality of the reads was assessed and reads with a quality score less than 20bp were trimmed out. The reads were then passed to the program Metaphlan (Segata et al. 2012) for primary identifications of microbial families included in the samples based on unique and clade-specific marker genes. In parallel to run Metaphlan analysis, we used BLAST program to map each read to the non-redundant nucleotide database of NCBI. We mapped the reads back to the bacterial genomes thought to be the pathogen; these are the top ranked bacteria based on Metaphlan, BLAST results, and related taxa analysis. The integration of the different tools and execution of the whole pipeline is achieved through python scripts developed in-house. A version of this pipeline is currently being imported to the workflow system Tavaxy (Abouelhoda et al. 2012) to be used by other researchers. Furthermore, we retrieved the genome annotation from the

Genbank and investigated the missing genes. In addition, we used QIIME the open-source bioinformatics pipeline for performing microbiome analysis from raw DNA sequencing data for taxonomic assignment and results visualizations (Caporaso et al. 2010).

Phylogenetic analysis

The 16S rDNA sequences of our isolate were used to construct a phylogenetic relationship with other *Proteus mirabilis* species. We acquired partial 16S rDNA sequences of selected *Proteus mirabilis* species from the GenBank. In order to establish the phylogenetic relationships among taxa, phylogenetic trees were constructed using the Maximum Likelihood (ML) method based on the Jukes-Cantor model the best fit to the data according to AIC criterion (Tamura and Nei 1993). MEGA6 (program / software/tool) was used to conduct phylogenetic analysis (Tamura et al. 2013, 0). In addition, a whole genome Neighbor-joining phylogenetic distance based tree of *Proteus mirabilis* spices including *Proteus mirabilis* SCDR1 isolate using the BLAST new enhanced graphical presentation and added functionality available at https://blast.ncbi.nlm.nih.gov/ (National Center for Biotechnology Information). In addition, we used Mauve (Darling et al. 2004) and CoCoNUT (Abouelhoda et al. 2008) to generate the whole genome pairwise and multiple alignments of the draft *P. mirabilis* strain SCDR1 genome against selected reference genomes. Furthermore, we performed whole genome phylogeny based proteomic comparison among *P. mirabilis* SCDR1 isolate and other related *Proteus mirabilis* strains using Proteome Comparison service which is protein sequence-based comparison using bi-directional BLASTP available at (https://www.patricbrc.org/app/SeqComparison) (Wattam et al. 2014).

Gene annotation and Pathogenomics analysis

P. mirabilis SCDR1 genome contigs were annotated using the Prokaryotic Genomes Automatic Annotation Pipeline (**PGAAP**) available at NCBI (http://www.ncbi.nlm.nih.gov/). In addition, contigs were further annotated using the bacterial bioinformatics database and analysis resource (**PATRIC**) gene annotation service (https://www.patricbrc.org/app/Annotation) (Wattam et al. 2014). The **PathogenFinder 1.1** pathogenicity prediction program available at

(https://cge.cbs.dtu.dk/services/PathogenFinder/) was used to examine the nature of *P. mirabilis* SCDR1 as a human pathogen (Cosentino et al. 2013). Virulence genes sequences and functions, corresponding to different major bacterial virulence factors of *Proteus mirabilis* were collected from GenBank and validated using virulence factors of pathogenic bacteria database available at (http://www.mgc.ac.cn/VFs/) (2003), Victors virulence factors search program available at (http://www.phidias.us/victors/) and PATRIC_VF tool available at https://www.patricbrc.org/portal/portal/patric/SpecialtyGeneSource?source=PATRIC_VF&kw= (Wattam et al. 2014).

Resistome analysis:

P. mirabilis SCDR1 genome contigs were investigated manually for the presence of antibiotic resistance loci using **PGAAP** and **PATRIC** gene annotation services. Antibiotic resistance loci were further investigated using specialized search tools and services namely, **Antibiotic Resistance Gene Search** available at (https://www.patricbrc.org/portal/portal/patric/AntibioticResistanceGeneSearch?cType=taxon&cId=131567&dm=) (Wattam et al. 2014), **Genome Feature Finder** (antibiotic resistance) available at (https://www.patricbrc.org/portal/portal/patric/GenomicFeature?cType=taxon&cId=131567&dm=) (Wattam et al. 2014), **ARDB** (Antibiotic Resistance Genes Database) available at (https://ardb.cbcb.umd.edu/) (Liu and Pop 2009), **CARD** (The Comprehensive Antibiotic Resistance Database) available at (https://card.mcmaster.ca/) (McArthur and Wright 2015; McArthur et al. 2013), **Specialty Gene Search** available at (https://www.patricbrc.org/portal/portal/patric/SpecialtyGeneSearch?cType=taxon&cId=131567&dm=) and **ResFinder 2.1** available at (https://cge.cbs.dtu.dk//services/ResFinder/) (Zankari et al. 2012).

The heavy metal resistance gene search *P. mirabilis* SCDR1 contigs were investigated using **PGAAP** and **PATRIC** gene annotation services, **PATRIC Feature Finder** searches tool and **BacMet**

(antibacterial biocide and metal resistance genes database) available at (http://bacmet.biomedicine.gu.se/) (Wattam et al. 2014; Pal et al. 2014).

Results:

Initial identification and Antimicrobial Susceptibility Test

The Vitek 2 system showed that our isolate belongs to *Proteus mirabilis* species. Antibiotic sensitivity testing using Vitek 2 AST-N204 card showed that our isolate *P. mirabilis* SCDR1 is resistant to ampicillin, nitrofurantoin, and Trimethoprim/ Sulfamethoxazole. In addition, *P. mirabilis* SCDR1 was resistant against ethidium Bromide, tetracycline, tigecycline, colistin, polymyxin B, rifamycin, doxycycline, vancomycin, fusidic acid, bacitracin, metronidazole, clarithromycin, erythromycin, oxacillin, clindamycin, trimethoprim, novobiocin, and minocycline. *P. mirabilis* SCDR1 was intermediate resistant against nalidixic acid, Imipenem, and Cefuroxime. Whereas it was sensitive to chloramphenicol, amoxicillin/ clavulanic Acid, piperacillin/tazobactam, cefotaxime, ceftazidime, cefepime, cefaclor, cephalothin, ertapenem, meropenem, amikacin, gentamicin, ciprofloxacin, norfloxacin, tobramycin, streptomycin, and fosfomycin.

P. mirabilis SCDR1 isolate showed high resistance against colloidal and composite Nanosilver and metallic silver compared with other tested Gram positive and negative bacterial species. For instance, **Table 1**, shows the resistance of *P. mirabilis SCDR1* against colloidal Nanosilver assessed by disk diffusion method in comparison with *S. aureus* ATCC 29213, *P. aeruginosa* ATCC 27853, *E. coli* ATCC 25922 and *E. cloacae* ATCC 29212. Generally, *P. mirabilis SCDR1* showed high resistance (0.0 cm), while *K. pneumoniae* showed the highest sensitivity (1.5-1.9 cm) against all tested silver nanoparticle concentrations (50-200 ppm). *S. aureus* also showed high sensitivity (1.4-1.6 cm) against all tested silver nanoparticle concentrations. None of the tested bacterial isolates, except for *P. mirabilis SCDR1*, showed any resistance against silver-nanoparticles even against the lowest concentration (50 ppm).

Table 1: Resistance of *P. mirabilis* SCDR1 against colloidal Nano-Silver assessed by desk diffusion method.

S. No.	Sample ID	Zone Of Inhibition (cm) *S. aureus*	Zone Of Inhibition (cm) *E. cloacae*	Zone Of Inhibition (cm) *P. aeruginosa*	Zone Of Inhibition (cm) *E. coli*	Zone Of Inhibition (cm) *K. pneumoniae*	Zone Of Inhibition (cm) *P. mirabilis* SCDR1
1	200 ppm	1.6 cm	1.5 cm	1.4 cm	1.1 cm	1.9 cm	0.0 cm
2	150 ppm	1.5 cm	1.2 cm	1.3 cm	1.0 cm	1.7 cm	0.0 cm
3	100 ppm	1.5 cm	1.2 cm	1.3 cm	1.0 cm	1.6 cm	0.0 cm
4	50 ppm	1.4 cm	1.1 cm	1.1 cm	0.9 cm	1.5 cm	0.0 cm

Furthermore, **Table 2** shows the resistance of *P. mirabilis* SCDR1 against colloidal Nanosilver assessed by minimal inhibitory concentration method compared with other tested Gram positive and negative bacterial species. Once more, *P. mirabilis SCDR1* showed high resistance against the gradually increased concentrations of colloidal Nano-Silver. We observed *P. mirabilis SCDR1* bacterial growth to colloidal Nanosilver concentration up to 500 ppm. On the other hand, *K. pneumoniae* showed the highest sensitivity against silver nanoparticles with no observed growth at only 100 ppm colloidal Nanosilver concentration. In addition, both *E. coli* and *P. aeruginosa* showed the high sensitivity against silver nanoparticles with no observed growth at 150 ppm colloidal Nanosilver concentration. While, *S. aureus* tolerated only 200 ppm colloidal Nanosilver concentration.

Similarly, **Table 3** shows the resistance of *P. mirabilis* SCDR1 against silver and Nanosilver composite assessed by disk diffusion method. Nanosilver chitosan composites, with concentration, ranged between 0.1% and 0.01M to 3.2% and 0.16M from chitosan and Silver nitrate respectively, had a comparable killing effect on both Gram positive and negative bacterial namely, *S. aureus* and *P. aeruginosa.* While none of the tested Nanosilver chitosan composites had any killing effect on *P. mirabilis* SCDR1. Similarly, all the tested commercially available silver and Nanosilver containing wound dressing bandages showed the enhanced killing effect on both *S. aureus* and *P. aeruginosa.* However, all these wound dressing bandages

failed to inhibit *P. mirabilis* SCDR1 growth. *P. mirabilis* SCDR1 was able to produce strong biofilm with OD of 0.296.

Table 2: Resistance of *P. mirabilis* SCDR1 against colloidal Nanosilver assessed by minimal inhibitory concentration method.

AgNPs (concentration in ppm)	Bacterial species/strain						
	***S. aureus* ATCC 29213**	***P. aeruginosa* ATCC 27853**	***E. cloacae* ATCC 29212**	***E. coli* ATCC 25922**	***K. pneumoniae* ATCC 700603**	***P. mirabilis* SCDR1**	***P. mirabilis* ATCC 29906**
50	Growth	Growth	Growth	Growth	Growth	Growth	Growth
100	Growth	Growth	Growth	Growth	No Growth	Growth	Growth
150	Growth	No Growth	Growth	No Growth	No Growth	Growth	Growth
200	Growth	No Growth	Growth	No Growth	No Growth	Growth	Growth
250	No Growth	No Growth	No Growth	No Growth	No Growth	Growth	Growth
300	No Growth	No Growth	No Growth	No Growth	No Growth	Growth	Growth
350	No Growth	No Growth	No Growth	No Growth	No Growth	Growth	Growth
400	No Growth	No Growth	No Growth	No Growth	No Growth	Growth	Growth
450	No Growth	No Growth	No Growth	No Growth	No Growth	Growth	Growth
500	No Growth	No Growth	No Growth	No Growth	No Growth	Growth	No Growth
550	No Growth	No Growth	No Growth	No Growth	No Growth	No Growth	No Growth
600	No Growth	No Growth	No Growth	No Growth	No Growth	No Growth	No Growth
650	No Growth	No Growth	No Growth	No Growth	No Growth	No Growth	No Growth
700	No Growth	No Growth	No Growth	No Growth	No Growth	No Growth	No Growth

Table 3: Resistance of *P. mirabilis* SCDR1 against silver and Nanosilver composite assessed by desk diffusion method.

Sample ID	Zone Of Inhibition (cm)	Zone Of Inhibition (cm)	Zone Of Inhibition (cm)
	S. aureus	***P. aeruginosa***	***P. mirabilis* SCDR1**
A	0.9 cm	0.8 cm	No. Inhibition
B	0.9 cm	0.9 cm	No. Inhibition
C	0.8 cm	0.9 cm	No. Inhibition
D	0.8 cm	0.9 cm	No. Inhibition
E	0.9 cm	0.9 cm	No. Inhibition
F	0.8 cm	0.8 cm	No. Inhibition
G	0.7 cm	0.7 cm	No. Inhibition
H	0.9 cm	0.9 cm	No. Inhibition
I	0.9 cm	1.0 cm	No. Inhibition

J	0.9 cm	1.0 cm	No. Inhibition
K	0.8 cm	0.6 cm	No. Inhibition
L	0.8 cm	0.8 cm	No. Inhibition
M	0.9 cm	0.8 cm	No. Inhibition
N	0.9 cm	0.9 cm	No. Inhibition
O	1.0 cm	0.9 cm	No. Inhibition
P	0.8 cm	0.8 cm	No. Inhibition
Q	0.9 cm	0.7 cm	No. Inhibition
R	0.9 cm	0.8 cm	No. Inhibition
S	0.8 cm	0.9 cm	No. Inhibition
T	1.0 cm	0.9 cm	No. Inhibition
U	0.8 cm	0.8 cm	No. Inhibition
V	0.9 cm	0.8 cm	No. Inhibition
W	0.9 cm	0.8 cm	No. Inhibition
X	1.0 cm	0.8 cm	No. Inhibition
Y	0.8 cm	0.8 cm	No. Inhibition
Z	0.7 cm	0.7 cm	No. Inhibition
A1	0.8 cm	0.7 cm	No. Inhibition
B2	0.9 cm	0.7 cm	No. Inhibition
C3	0.9 cm	0.8 cm	No. Inhibition
D4	0.6 cm	NA	No. Inhibition
Silvercel	1.3 cm	1.4 cm	No. Inhibition
Sorbsan silver	1.9 cm	2.0 cm	No. Inhibition
Colactive® Plus Ag	1.5cm	2.0cm	No. Inhibition
Exsalt™ SD7	1.5cm	1.5cm	No. Inhibition
Puracol ® Plus Ag	1.4cm	2.0cm	No. Inhibition
Actisorb® Silver 220	0.9cm	1.2cm	No. Inhibition

General genome features.

Data from our draft genome of *P. mirabilis* SCDR1 was deposited in the NCBI-GenBank and was assigned accession number LUFT00000000. The *P. mirabilis* SCDR1 assembly resulted in 63 contigs, with an N50 contig size of 227,512 bp nucleotides, and a total length of 3,815,621 bp. The average G+C content was 38.44%. Contigs were annotated using the Prokaryotic Genomes Automatic Annotation Pipeline (PGAAP) available at NCBI (http://www.ncbi.nlm.nih.gov/) providing a total of 3,533 genes, 3,414 coding DNA sequence genes, 11, 10, 18 rRNAs (5S, 16S, and 23S), and 76 tRNAs. On the other hand, the bacterial bioinformatics database and analysis resource (PATRIC) gene annotation analysis showed that the number of the observed coding sequence (CDS) is 4423, rRNA is 10 and tRNA is 71. The unique gene count for the different observed metabolic pathways is 2585 (**Figure 1**).

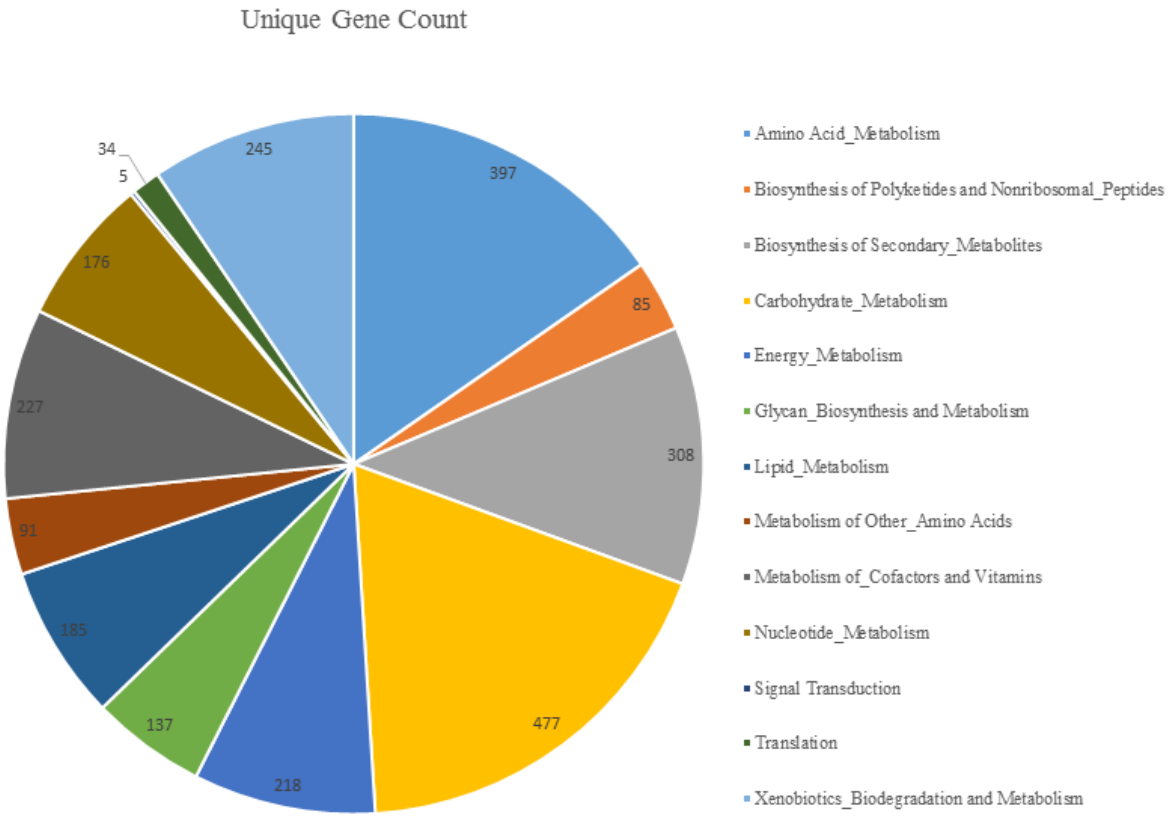

Figure 1: Distribution of unique gene counts amongst different metabolic pathways.

Carbohydrate metabolism pathways maintained the highest number of dedicated unique gene count (477) while signal transduction pathways maintained the highest number (5). In addition, biosynthesis of secondary metabolites, such as tetracycline, Streptomycin, Novobiocin, and Betalain, maintained a high number of dedicated unique gene (308). It is also noteworthy that Xenobiotics Biodegradation and Metabolism pathways also maintained a high number of dedicated unique gene (245) (**Supplementary table 1 and 2**).

Pathogen identification and phylogenetic analysis.

As stated before biochemical identification of the isolate confirmed the identity of our isolate to be belonging to *Proteus mirabilis* species. Moreover, Primary analysis of Metaphlan showed that *Proteus mirabilis* is the most dominant species in the sample (**Figure 2**). The appearance of other bacterial species in the Metaphlan diagram is explained by genomic homology similarity of other bacteria to *Proteus mirabilis.* *P. mirabilis* SCDR1 genome showed high similarly 92.07% to the genome of *P. mirabilis* strain BB2000 followed by *P. mirabilis* strain C05028 (90.99%) and *P. mirabilis* strain PR03 (89.73%) (**Table 4**).

A similar scenario was observed when constructing the phylogenetic relationship between our isolate and other *Proteus mirabilis* available in the NCBI- GenBank. 16Sr DNA-based maximum likelihood phylogenetic tree (**Figure 3**) showed that our isolate is located within a large clade that contains the majority of *Proteus mirabilis* strains and isolates. In addition, *P. mirabilis* SCDR1 showed to be closely related to the reference strain *P. mirabilis* HI4320 compared with *P. mirabilis* BB2000 that is located in another clade of four Proteus *mirabilis* taxa. On the contrary, whole genome Neighbor-joining phylogenetic tree of *Proteus mirabilis* spices including *P. mirabilis* SCDR1 isolate (**Figure 4**), showed that our isolate is more closely related to *P. mirabilis* BB2000 compared with the reference strain/genome *P. mirabilis* HI4320. However, Figure 4 showed that *P. mirabilis* SCDR1 exhibited obvious genetic divergence from other *Proteus mirabilis* species. Similar results were observed when performing pairwise pair-wise whole genome alignment of *P. mirabilis* strain SCDR1 against reference genomes **(Figure 5)**.

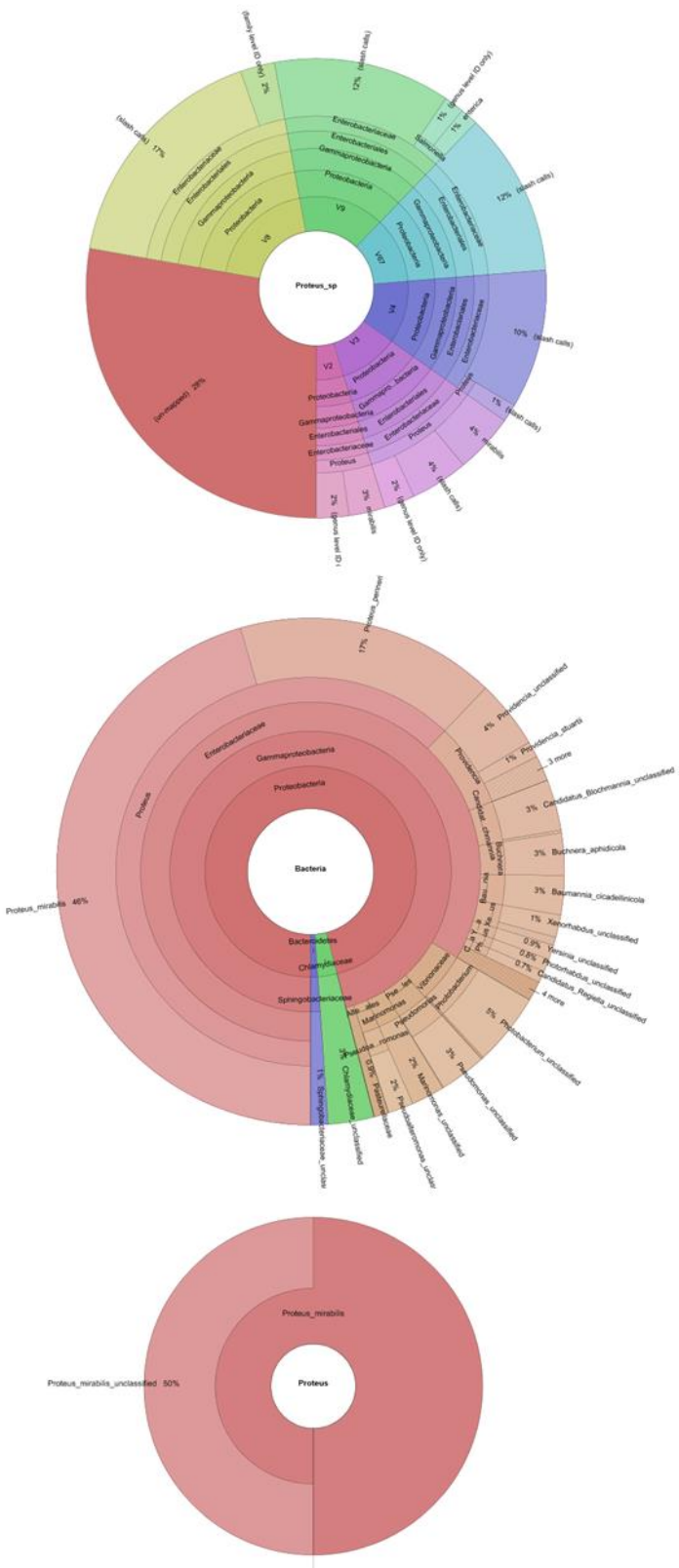

291

292 **Figure 2: Metaphlan primary identification of the tested taxon.**

293 **Table 4: Comparison of *Proteus mirabilis* SCDR1 to complete and draft reference genomes of *Proteus mirabilis.***

Completed Genomes							
NCBI ID	**Reference**	**Ref Size**	**Gaps sum length**	**Gaps >= 100 bp**	**Bases sum length**	**Bases > 500 bp**	**% Reference**
NC_010554.1	*Proteus mirabilis* HI4320	4,063,606	555,251	549,285	3,508,355	3,472,919	86.33
NC_010555.1	*Proteus mirabilis* plasmid pHI4320	36,289	36,289	36,289	0	0	0
NC_022000.1	Proteus mirabilis BB2000	3,846,754	304,708	298,947	3,542,046	3,510,682	92.07
Draft Genomes							
NCBI ID	**Reference**	**Ref Size**	**Gaps sum length**	**Gaps >= 100 bp**	**Bases sum length**	**Bases > 500 bp**	**% Reference**
NZ_ACLE00000000	*Proteus mirabilis* ATCC_29906	4,027,100	565,180	560,679	3,461,920	3,432,786	85.96
NZ_ANBT00000000	*Proteus mirabilis* C05028	3,817,619	343,688	338,218	3,473,931	3,445,432	90.99
NZ_AORN00000000	*Proteus mirabilis* PR03	3,847,612	394,926	390,203	3,452,686	3,430,536	89.73
NZ_AMGU00000000	*Proteus mirabilis* WGLW4	3,960,485	474,704	469,864	3,485,781	3,458,264	88.01
NZ_AMGT00000000	*Proteus mirabilis* WGLW6	4,101,891	606,773	601,555	3,495,118	3,461,467	85.20

294

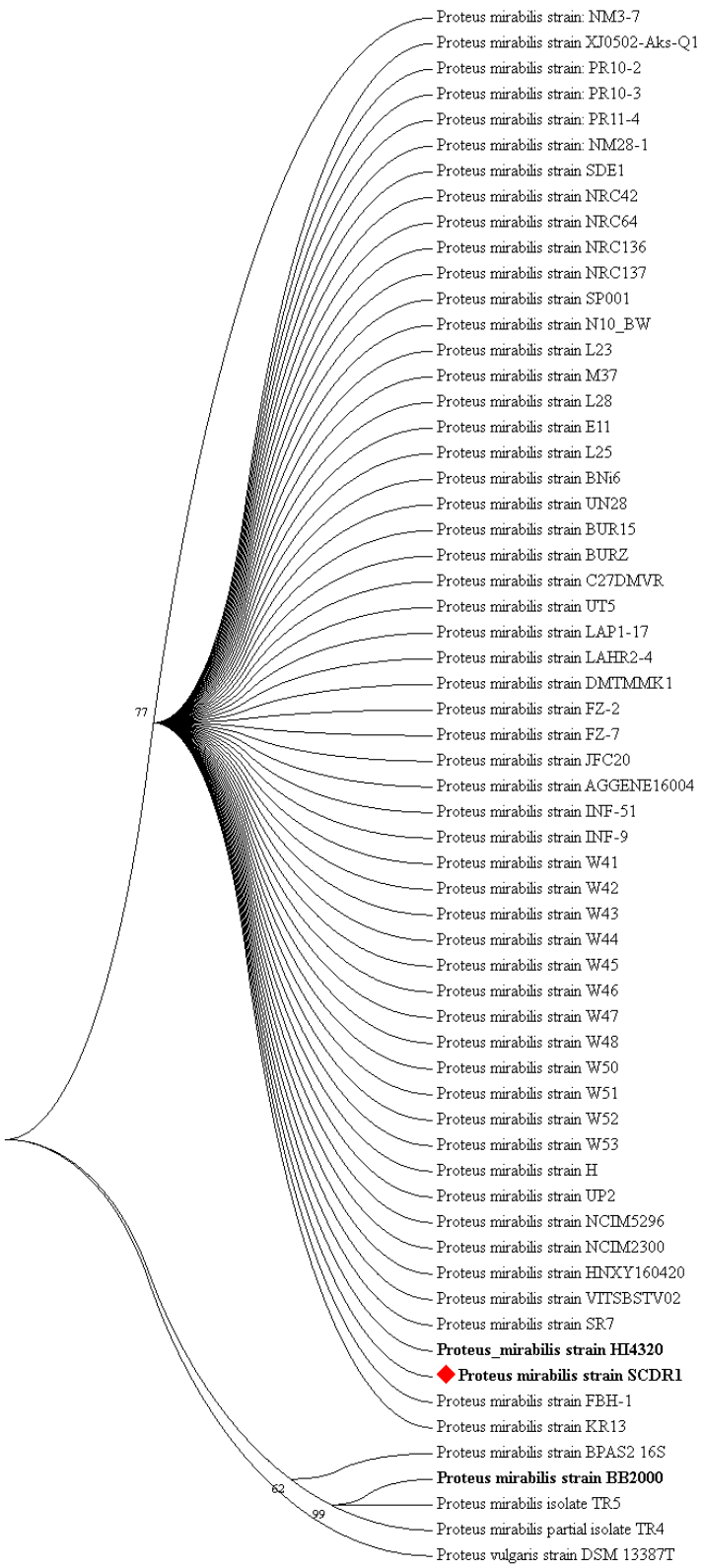

Figure 3: 16S rDNA based Maximum likelihood phylogenetic tree of Proteus mirabilis spices including Pm-SCDR1 isolate.

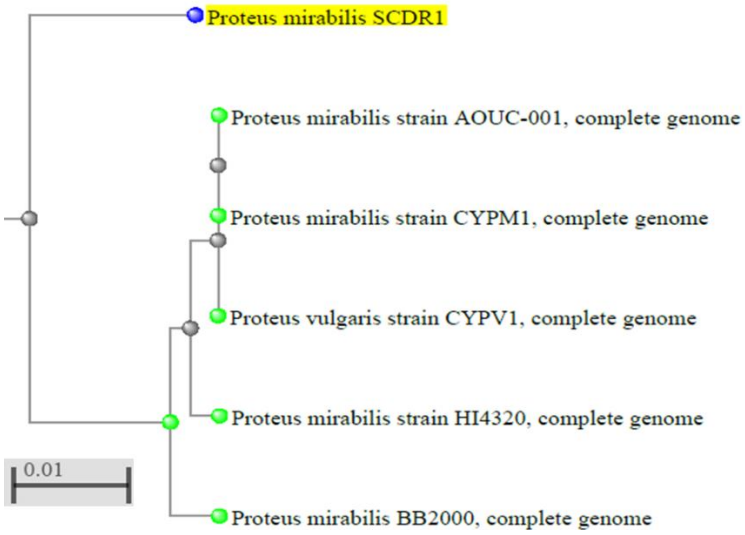

Figure 4: Whole genome Neighbor joining phylogenetic tree of *Proteus mirabilis* spices including Pm-SCDR1 isolate.

This was also confirmed with the clear divergence among *P. mirabilis* SCDR1 *Proteus mirabilis* species on the proteomic level (**Figure 6**). Comparing annotated proteins across genomes showed that the majority of protein sequence identity ranged between 95-99.5% with the highest values (100%) was observed for ribosomal proteins such as, SSU ribosomal protein S10p (S20e), LSU ribosomal protein L3p (L3e), LSU ribosomal protein L4p (L1e), and energy production involved proteins such as, ATP synthase gamma chain, beta chain and epsilon chain, cell division proteins such as, Cell division protein FtsZ, FtsA and FtsQ, NADH-ubiquinone oxidoreductase chains K, J, I, H and G and some other conserved essential proteins. On the other hand low values of protein identity similarities (26-85%) were observed for some proteins such as Fimbriae related proteins, transcriptional regulators, Ribosomal large subunit pseudouridine synthases, Phage-related proteins, O-antigen acetylases, inner and outer membrane-related proteins, secreted proteins, heavy metal transporting ATPases, Drug resistance efflux proteins, Iron transport proteins and cell invasion proteins.

315 Figure 5 (a)

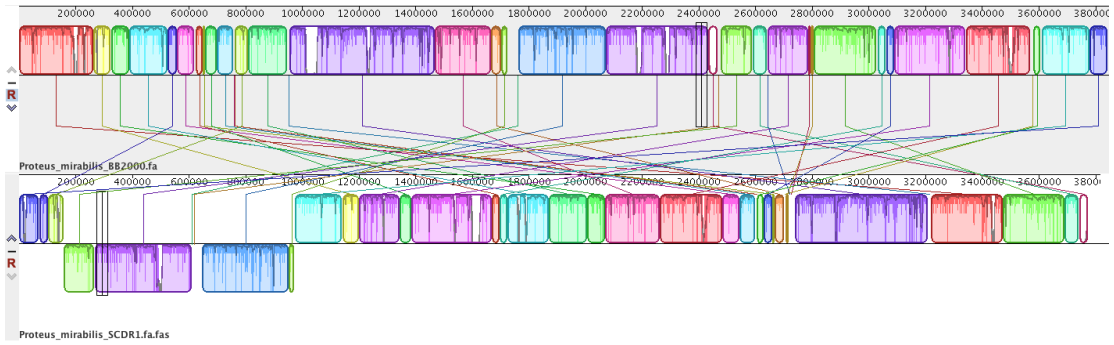

316

317

318 Figure 5 (b)

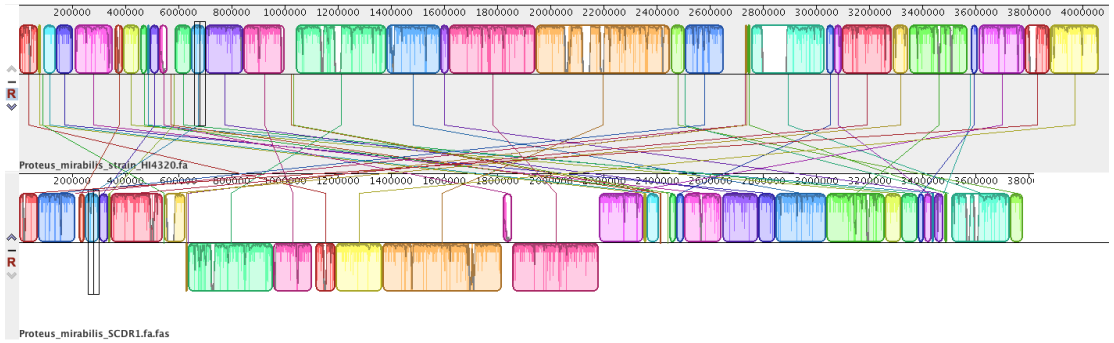

319

320

321 Figure 5 (c)

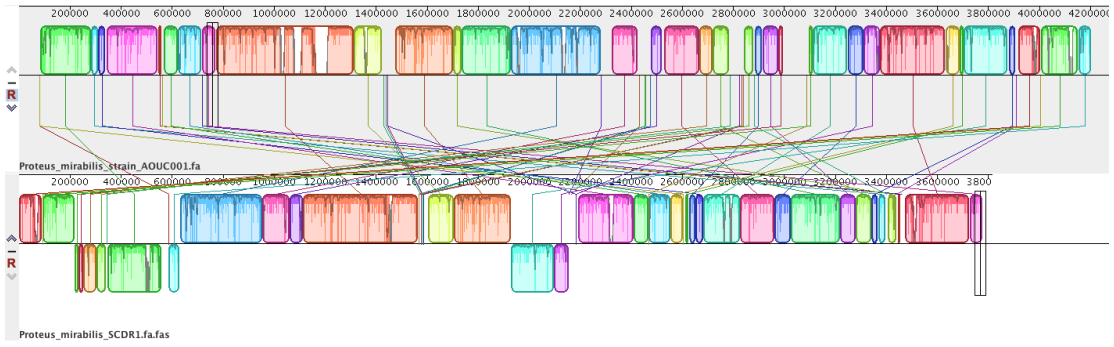

322

323

324

325

Figure 5 (d):

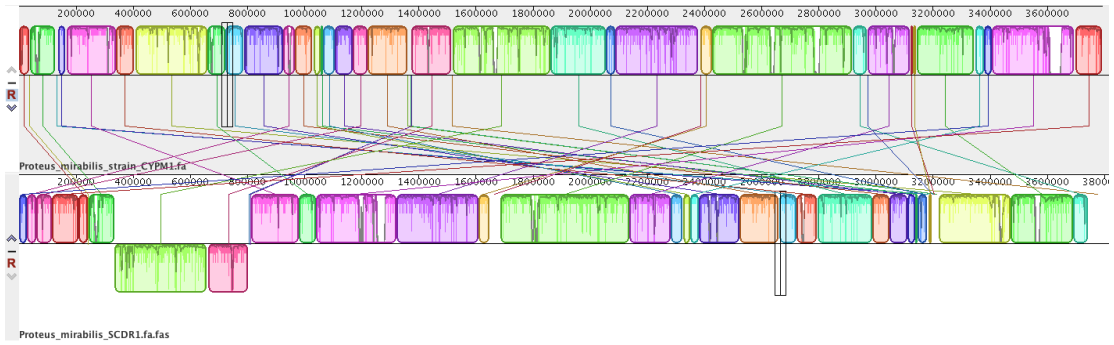

Figure 5 (e):

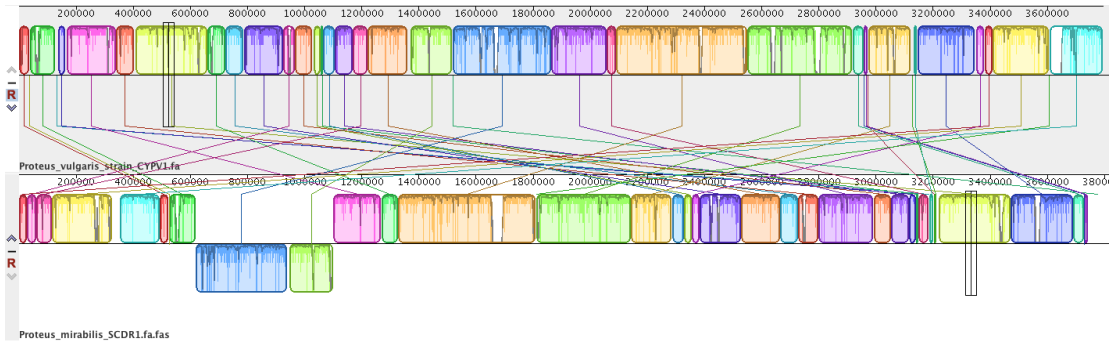

Figure 5 (f):

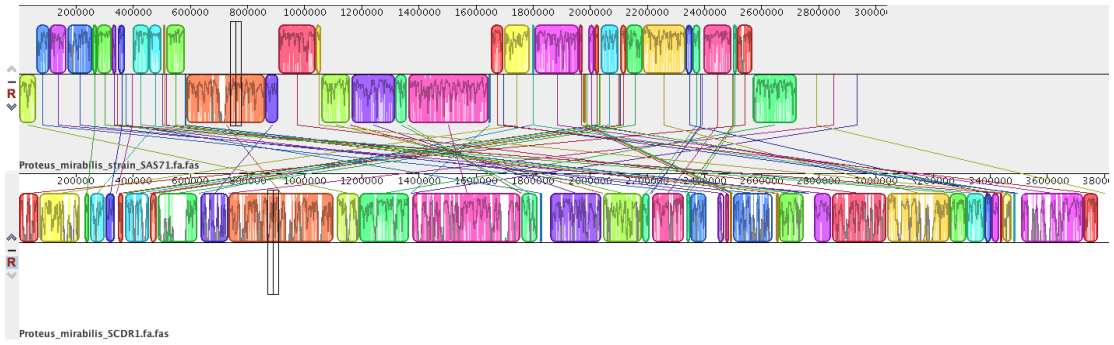

Figure 5: Pair-wise Whole Genome Alignment of *P. mirabilis* strain SCDR1 against reference genomes. (a) *P. mirabilis BB200* and *P. mirabilis* SCDR1, (b) *P. mirabilis HI4320* and *P. mirabilis* SCDR1, (c) *P. mirabilis* AOUC001 and *P. mirabilis* SCDR1, (d) *P. mirabilis* CYPM1 and *P. mirabilis* SCDR1, (e) *P. vulgaris* CYPV1 and *P. mirabilis* SCDR1 and (f) *P. mirabilis* SAS71 and *P. mirabilis* SCDR1 Mauve whole genome alignment.

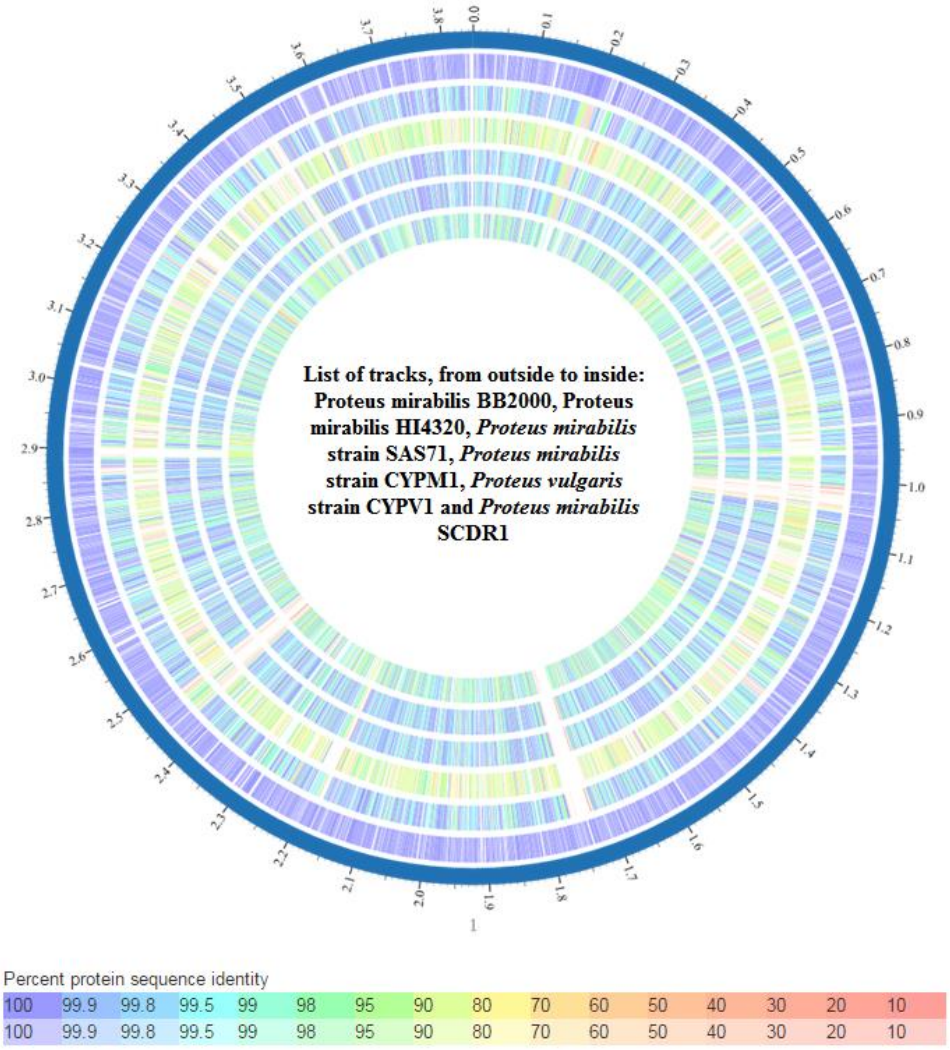

Figure 6: Whole genome phylogeny based proteomic comparison among *Proteus mirabilis* strains.

Bacterial pathogenic and virulence factors

Pathogenomics analysis using PathogenFinder 1.1 showed that our input organism was predicted as a human pathogen, Probability of being a human pathogen 0.857. *P. mirabilis* SCDR1 comparative proteome analysis showed 35 matched hits from pathogenic families and only one hit from non-pathogenic families (**Supplementary Table 3**). In addition, genome analysis showed that *P. mirabilis* SCDR1 isolate contains numerous virulence factor genes and/or operons that marques it to be a virulent pathogenic bacterium. These virulence factors include Swarming behavior, mobility (flagellae), adherence, toxin and hemolysin production, Urease, Quorum sensing, iron acquisition systems, proteins that function in immune evasion,

cell invasion and biofilm formation, stress tolerance factors, and chemotaxis related factors (**Supplementary Table 4**).

Proteus mirabilis SCDR1 Resistome:

Antibiotic resistance:

Antibiotic resistance identification Perfect and Strict analysis using Resistance Gene Identifier (RGI) showed that *P. mirabilis* SCDR1 isolate contains 34 antibiotic resistance genes that serve in 21 antibiotic resistance functional categories (**Supplementary Table 5 and Figure 7**). **Table 5** displays the consensus *P. mirabilis*-SCDR1 antibiotic resistome. Genomics analysis of *P. mirabilis*-SCDR1 63 contigs showed that our isolates contains genetic determinants for tetracycline resistance (tetAJ), fluoroquinolones resistance (gyrA, parC and parE), sulfonamide resistance (folP), daptomycin and rifamycin resistance (rpoB), elfamycin antibiotics resistance (tufB), Chloramphenicol (cpxR, cpxA and cat), Ethidium bromide-methyl viologen resistance protein (emrE) and Polymyxin resistance (phoP). In addition, several multidrug resistance efflux systems and complexes such as MdtABC-TolC, MacAB-TolC, AcrAB-TolC, EmrAB-TolC, AcrEF-TolC and MATE.

Heavy metal resistance:

Table 6 presents *P. mirabilis* SCDR1 Heavy Metal Resistance/Binding factors. Numerous genetic determinants for metal resistance were observed in *P. mirabilis* SCDR1 genome. Several Copper resistance genes/proteins were detected, namely, copA, copB, copC, copD, cueO, cueR, cutC, cutF and CuRO_2_CopA_like1. In addition, gene determinants of Copper/silver efflux system were also observed, namely, oprB, oprM and cusC_1. Moreover, several heavy metal resistance proteins and efflux systems were also observed such as magnesium/cobalt efflux protein CorC, metal resistance proteins (AGS59089.1, AGS59090.1 and AGS59091.1), nickel-cobalt-cadmium resistance protein NccB, arsenical pump membrane protein (ArsB permease), Lead, cadmium, zinc and mercury transporting ATPase, outer membrane component of tripartite multidrug resistance system (CusC) and complete *P. mirabilis* tellurite resistance loci (terB, terA, terC, terD, terE, terZ). Furthermore, enzymes involved in heavy metal resistance

were also observed such as Glutathione S-transferase (gst1, gst, Delta and Uncharacterized), arsenite S-adenosylmethyltransferase (Methyltransferase type 11) and alkylmercury lyase (MerB).

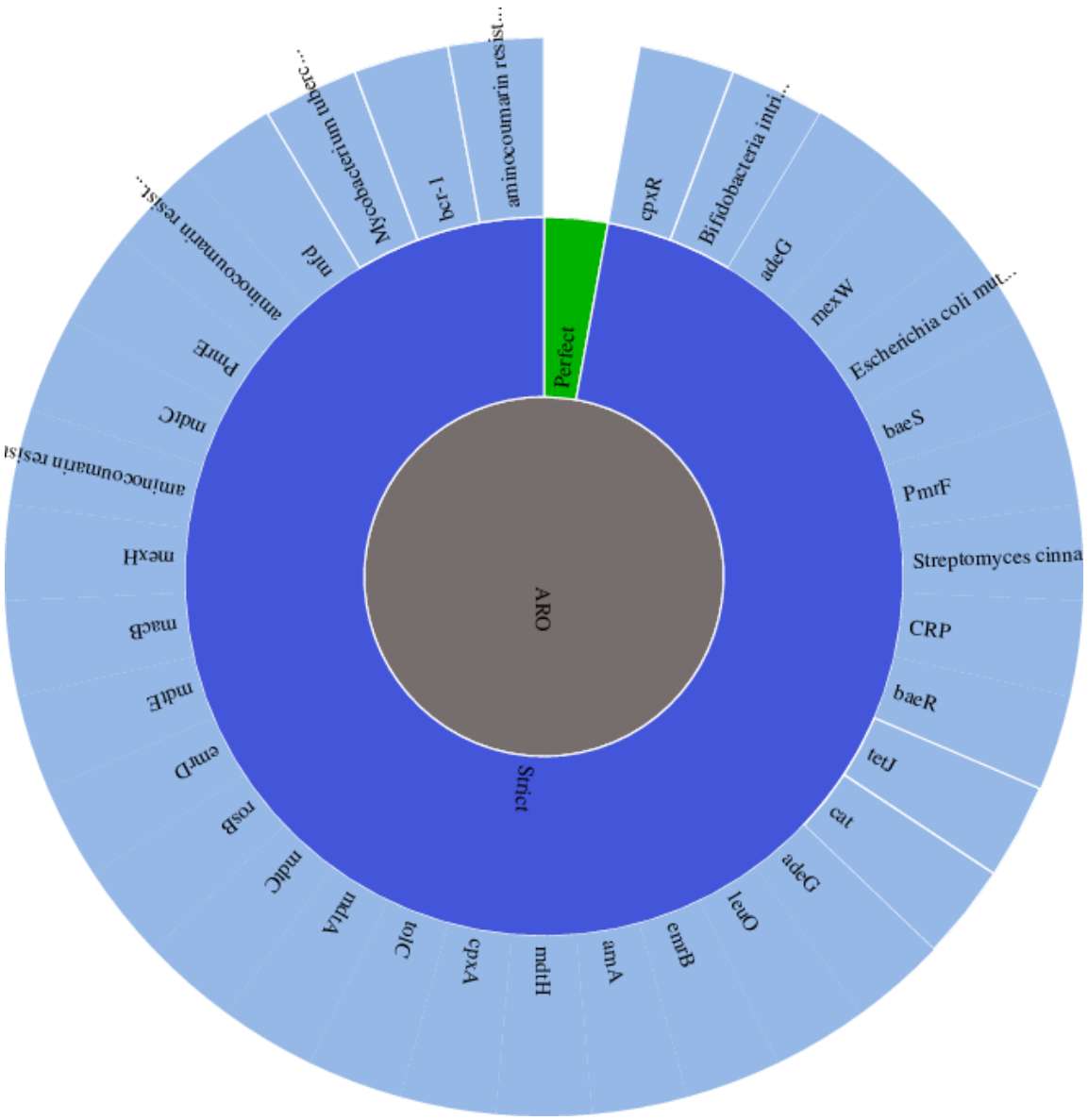

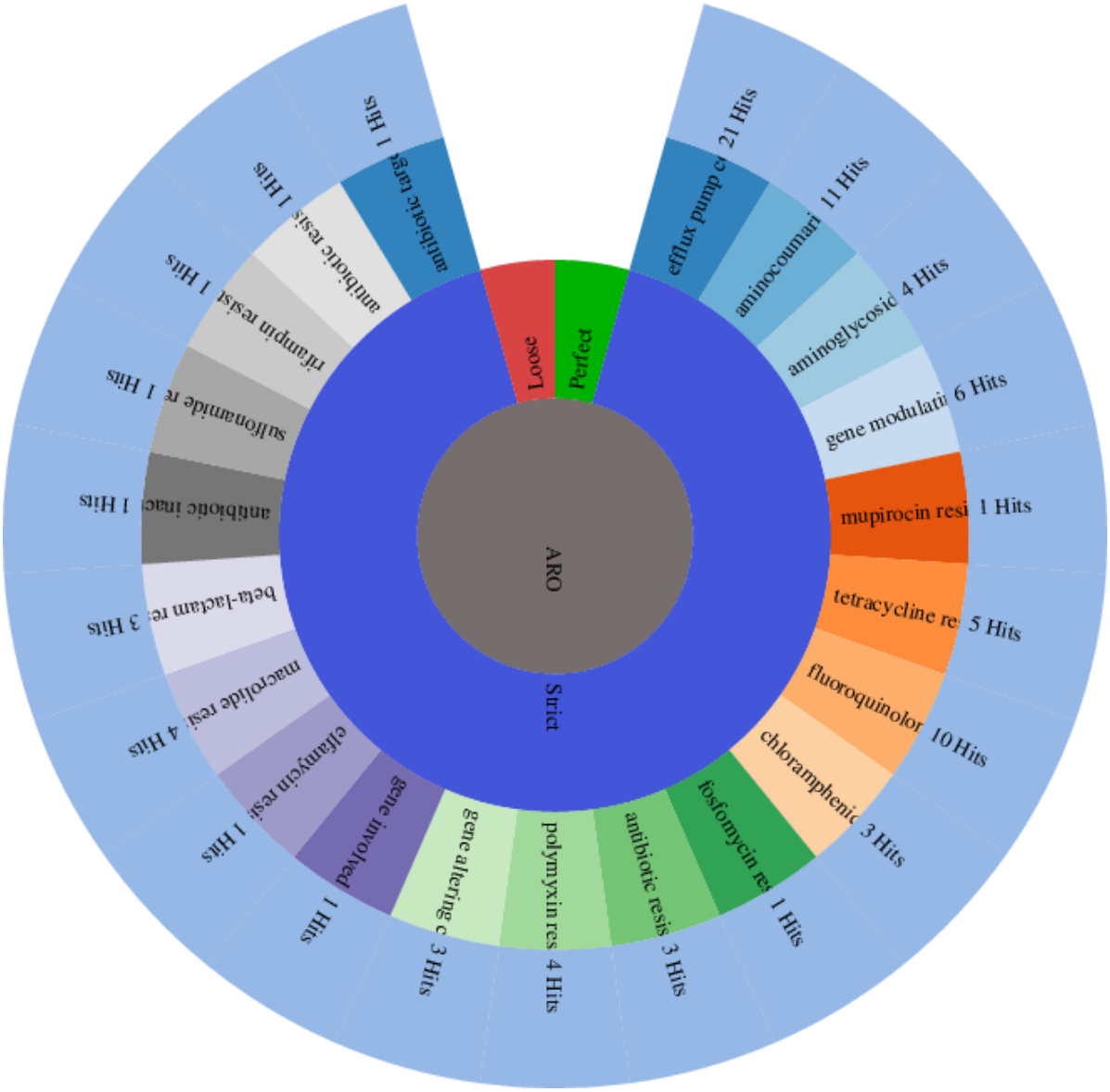

Figure 7: Antibiotic Resistance strict gene analysis and function analysis for *Proteus mirabilis* SCDR1.

385 **Table 5: Consensus *P. mirabilis*-SCDR1 antibiotic Resistome.**

Source	Source Organism	Gene	Product	Function	Query Coverage	Identity	E-value
ARDB	*P. mirabilis* ATCC 29906	tetAJ	Tetracycline efflux protein TetA	Major facilitator superfamily transporter, tetracycline efflux pump.	97	95	0
CARD	*P. mirabilis* BB2000	tetAJ	Tetracycline efflux protein TetA	Major facilitator superfamily transporter, tetracycline efflux pump.	97	94	0
ARDB	*P. mirabilis* HI4320	tetAJ	Tetracycline efflux protein TetA	Major facilitator superfamily transporter, tetracycline efflux pump.	80	99	2e-74
CARD	*P. mirabilis* BB2000	gyrA	DNA gyrase subunit A (EC 5.99.1.3)	Point mutation of Escherichia coli gyrA resulted in the lowered affinity between fluoroquinolones and gyrA. Thus, conferring resistance	98	99	0
CARD	*P. mirabilis* BB2000	baeR	Response regulator BaeR	BaeR is a response regulator that promotes the expression of MdtABC and AcrD efflux complexes.	100	99	2e-171
CARD	*P. mirabilis* BB2000	baeS	Sensory histidine kinase BaeS	BaeS is a sensor kinase in the BaeSR regulatory system. While it phosphorylates BaeR to increase its activity.	100	99	0
CARD	*P. mirabilis* BB2000	mdtC	Multidrug transporter MdtC	MdtC is a transporter that forms a hetero-multimer complex with MdtB to form a multidrug transporter. MdtBC is part of the MdtABC-TolC efflux complex.	100	99	0
CARD	*P. mirabilis* BB2000	mdtB	Multidrug transporter MdtB	MdtB is a transporter that forms a heteromultimer complex with MdtC to form a multidrug transporter. MdtBC is part of the MdtABC-TolC efflux complex.	100	99	0
CARD	*P. mirabilis* BB2000	mdtA	RND efflux system, membrane fusion protein	MdtA is the membrane fusion protein of the multidrug efflux complex mdtABC.	100	98	0
CARD	*P. mirabilis* BB2000	folP	Dihydropteroate synthase (EC 2.5.1.15)	Point mutations in dihydropteroate synthase folP prevent sulfonamide antibiotics from inhibiting its role in folate synthesis, thus conferring sulfonamide resistance.	100	100	0
CARD	*P. mirabilis* BB2000	soxR	Redox-sensitive transcriptional activator SoxR	SoxR is a sensory protein that upregulates soxS expression in the presence of redox-cycling drugs. This stress response leads to the expression many multidrug efflux pumps.	100	100	0
CARD	*Shigella dysenteriae* Sd197	ompR	Two-component system response regulator OmpR	Transcriptional regulatory protein	99	87	0
CARD	*P. mirabilis* BB2000	emrR	Transcriptional repressor MprA	EmrR is a negative regulator for the EmrAB-TolC multidrug efflux pump in E. coli. Mutations lead to EmrAB-TolC overexpression.	100	100	0
CARD	*P. mirabilis* BB2000	emrA	Multidrug resistance protein ErmA	EmrA is a membrane fusion protein, providing an efflux pathway with EmrB and TolC between the inner and outer membranes of E. coli, a Gram-negative bacterium.	95	96	0
CARD	*P. mirabilis* BB2000	acrE	Membrane fusion component of tripartite multidrug resistance system	AcrEF-TolC is a tripartite multidrug efflux system similar to AcrAB-TolC and found in Gram-negative bacteria. AcrE is the membrane fusion protein, AcrF is the inner membrane transporter, and TolC is the outer membrane channel protein.	100	98	3e-44
CARD	*P. mirabilis* BB2000	emrB	Multidrug resistance protein ErmB	emrB is a translocase in the emrB -TolC efflux protein in E. coli. It recognizes substrates including carbonyl cyanide m-chlorophenylhydrazone (CCCP), nalidixic acid, and thioloactomycin.	100	99	0
CARD	*P. mirabilis* BB2000	rpoB	DNA-directed RNA polymerase beta subunit (EC 2.7.7.6)	Mutations in rpoB gene confers antibiotic resistance (Daptomycin and Rifamycin)	100	99	0

CARD	*P. mirabilis* BB2000	tufB	Translation elongation factor Tu	Sequence variants of elongation factor Tu confer resistance to elfamycin antibiotics.	100	100	1e-43
CARD	*P. mirabilis* BB2000	cpxA	Copper sensory histidine kinase CpxA	cpxA mutant confer resistant to amikacin	94	99	0
CARD	*P. mirabilis* BB2000	cpxR	Copper-sensing two-component system response regulator CpxR	CpxR is a regulator that promotes acrD expression when phosphorylated by a cascade involving CpxA, a sensor kinase. cefepime and chloramphenicol	100	100	0
CARD	*P. mirabilis* BB2000	emrD	Multidrug resistance protein D	EmrD is a multidrug transporter from the Major Facilitator Superfamily (MFS) primarily found in Escherichia coli. EmrD couples efflux of amphipathic compounds with proton import across the plasma membrane.	100	99	0
CARD	*P. mirabilis* BB2000	macA	Macrolide-specific efflux protein MacA	MacA is a membrane fusion protein that forms an antibiotic efflux complex with MacB and TolC.	100	99	3e-177
CARD	*P. mirabilis* BB2000	macB	Macrolide export ATP-binding/permease protein MacB (EC 3.6.3.-)	MacB is an ATP-binding cassette (ABC) transporter that exports macrolides with 14- or 15- membered lactones. It forms an antibiotic efflux complex with MacA and TolC.	100	98	0
ARDB	*P. mirabilis* ATCC 29906	cat	Chloramphenicol acetyltransferase (EC 2.3.1.28)	Group A chloramphenicol acetyltransferase, which can inactivate chloramphenicol.	99	93	6e-150
CARD	*P. mirabilis* BB2000	cat	Chloramphenicol acetyltransferase (EC 2.3.1.28)	Group A chloramphenicol acetyltransferase, which can inactivate chloramphenicol.	99	93	4e-151
CARD	*P. mirabilis* BB2000	acrR	Transcription repressor of multidrug efflux pump acrAB operon, TetR (AcrR) family	AcrR is a repressor of the AcrAB-TolC multidrug efflux complex. AcrR mutations result in high level antibiotic resistance.	100	95	9e-25
CARD	*P. mirabilis* BB2000	acrR	Transcriptional regulator of acrAB operon, AcrR	AcrR is a repressor of the AcrAB-TolC multidrug efflux complex. AcrR mutations result in high level antibiotic resistance.	93	95	2e-114
CARD	*P. mirabilis* BB2000	acrA	RND efflux system, membrane fusion protein	Protein subunit of AcrA-AcrB-TolC multidrug efflux complex. AcrA represents the periplasmic portion of the transport protein.	100	99	0
CARD	*P. mirabilis* BB2000	mdtK	Multi antimicrobial extrusion protein (Na(+)/drug antiporter), MATE family of MDR efflux pumps	A multidrug and toxic compound extrusions (MATE) transporter conferring resistance to norfloxacin, doxorubicin and acriflavine.	98	99	3e-164
CARD	*Salmonella enterica subsp. enterica serovar Agona* str. SL483	hns	DNA-binding protein H-NS	H-NS is a histone-like protein involved in global gene regulation in Gram-negative bacteria. It is a repressor of the membrane fusion protein genes acrE, mdtE, and emrK as well as nearby genes of many RND-type multidrug exporters.	100	80	0
CARD	*P. mirabilis* BB2000	tufB	Translation elongation factor Tu	Sequence variants of elongation factor Tu confer resistance to elfamycin antibiotics.	100	99	0
CARD	*Shigella dysenteriae* Sd197	crp	Cyclic AMP receptor protein	CRP is a global regulator that represses MdtEF multidrug efflux pump expression.	100	98	0
CARD	*P. mirabilis* BB2000	emrE	Ethidium bromide-methyl viologen resistance protein EmrE	EmrE is a small multidrug transporter that functions as a homodimer and that couples the efflux of small polyaromatic cations from the cell with the import of protons down an electrochemical gradient. EmrE is found in E. coli and P. aeruginosa.	100	99	6e-73
CARD	*P. mirabilis* BB2000	mdtK	Multi antimicrobial extrusion protein (Na(+)/drug antiporter), MATE family of MDR efflux pumps	A multidrug and toxic compound extrusions (MATE) transporter conferring resistance to norfloxacin, doxorubicin and acriflavine.	100	100	2e-113

CARD	*P. mirabilis* BB2000	NIA	Putative transport protein	NIA	100	94	7e-59
CARD	*P. mirabilis* BB2000	NIA	Multidrug resistance protein	NIA	99	96	2e-112
CARD	*P. mirabilis* BB2000	parC	Topoisomerase IV subunit A (EC 5.99.1.-)	ParC is a subunit of topoisomerase IV, which decatenates and relaxes DNA to allow access to genes for transcription or translation. Point mutations in ParC prevent fluoroquinolone antibiotics from inhibiting DNA synthesis, and confer low-level resistance. Higher-level resistance results from both gyrA and parC mutations.	99	99	0
CARD	*P. mirabilis* BB2000	parE	Topoisomerase IV subunit B (EC 5.99.1.-)	ParE is a subunit of topoisomerase IV, necessary for cell survival. Point mutations in ParE prevent fluoroquinolones from inhibiting DNA synthesis, thus conferring resistance.	100	99	0
CARD	*P. mirabilis* BB2000	tolC	Type I secretion outer membrane protein, TolC precursor	TolC is a protein subunit of many multidrug efflux complexes in Gram negative bacteria. It is an outer membrane efflux protein and is constitutively open. Regulation of efflux activity is often at its periplasmic entrance by other components of the efflux complex.	100	99	0
CARD	*P. mirabilis* BB2000	mdtH	MFS superfamily export protein YceL	Multidrug resistance protein MdtH	100	99	0
CARD	*P. mirabilis* BB2000	phoP	Transcriptional regulatory protein PhoP	A mutant phoP activates pmrHFIJKLM expression responsible for L-aminoarabinose synthesis and polymyxin resistance, by way of alteration of negative charge	100	99	5e-165
CARD	*P. mirabilis* BB2000	phoQ	Sensor histidine kinase PhoQ (EC 2.7.13.3)	Mutations in Pseudomonas aeruginosa PhoQ of the two-component PhoPQ regulatory system. Presence of mutation confers resistance to colistin	90	99	0
CARD	*P. mirabilis* BB2000	phoQ	Sensor histidine kinase PhoQ (EC 2.7.13.3)	Mutations in Pseudomonas aeruginosa PhoQ of the two-component PhoPQ regulatory system. Presence of mutation confers resistance to colistin	98	98	1e-45

Evidence: BLASTP, **NIA**: No information available, **ARDB:** Antibiotic Resistance Genes Database, **CARD:** Comprehensive Antibiotic Resistance Database.

395 **Table 6: *P. mirabilis* SCDR1 Heavy Metal Resistance/Binding factors.**

Annotation	Reference Genome	Accession Number	Gene	Protein ID	AA Length	Corresponding Protein
PATRIC	*P. mirabilis* ATCC 29906	NZ_GG668580	corC	ZP_03842837.1	293	Magnesium/cobalt efflux protein CorC.
RefSeq	*P. mirabilis* BB2000	CP004022	NA	AGS60530.1	305	cation efflux protein (Divalent metal cation (Fe/Co/Zn/Cd) transporter).
PATRIC	*P. mirabilis* ATCC 29906	NZ_GG668576	cueR	ZP_03840921.1	133	MerR-family transcriptional regulator (copper efflux regulator).
RefSeq	*P. mirabilis* BB2000	CP004022	arsB	AGS60689.1	429	Arsenical pump membrane protein (ArsB_permease).
RefSeq	*P. mirabilis* BB2000	CP004022	NA	AGS59089.1 AGS59090.1 AGS59091.1	129 678 243	Metal resistance protein.
PATRIC	*P. mirabilis* ATCC 29906 *P. mirabilis* strain 25933 GTA	NZ_GG668576 LANL01000027	ahpF NA	ZP_03839875.1 KKC60389.1	521 678	Protein-disulfide reductase.
PATRIC	*P. mirabilis* ATCC 29906	NZ_GG668576 NZ_GG668583	dsbB dsbA	ZP_03840198.1 ZP_03839563.1	174 207	Protein disulfide oxidoreductase.
PATRIC	*P. mirabilis* ATCC 29906 *P. mirabilis* BB2000	NZ_GG668576 NZ_GG668576 NZ_GG668578 CP004022	actP1 copA ppaA zntA	ZP_03840801.1 ZP_03840922.1 ZP_03842696.1 AGS58561.1	829 984 803 796	(zinc/cadmium/mercury/lead-transporting ATPase) (HMA).
PATRIC	*P. mirabilis* ATCC 29906	NZ_GG668578	gloB	ZP_03842342.1	251	hydroxyacylglutathione hydrolase.
RefSeq	*P. mirabilis* strain ATCC 7002	JOVJ01000008	grxA	KGA90223.1	87	Glutaredoxin, GrxA family.
PATRIC	*P. mirabilis* ATCC 29906 *P. mirabilis* strain 1134_PMIR	NZ_GG668576 NZ_GG668576	gst1 gst Delta Uncharacterized	ZP_03840532.1 ZP_03840063.1 PGF_02913068* PGF_00008413*	204 203 195 110	Glutathione S-transferase (EC 2.5.1.18).
RefSeq	*P. mirabilis* BB2000	CP004022	cueO	AGS58840.1	526	Multicopper oxidase.
PATRIC	*P. mirabilis* ATCC 29906	NZ_GG668578	NA	ZP_03842149.1	243	FIG00003370: Multicopper polyphenol oxidase.
PATRIC	*P. mirabilis* strain ATCC 7002	JOVJ01000009	yobA	ZP_03839688.1	130	Copper resistance protein (Copper-binding protein CopC (methionine-rich)) [Inorganic ion transport and metabolism].
PATRIC	*P. mirabilis* ATCC 29906	NZ_GG668576	copD	ZP_03839689.1	279	Copper resistance protein.
PATRIC	*P. mirabilis* strain SAS71	LDIU01000481	NA	PGF_00419563	114	Copper resistance protein D.
BRC1	*P. mirabilis* HI4320	NC_010554	NA	NA	300	Putative copper resistance protein, secreted.
PATRIC RefSeq	*P. mirabilis* ATCC 29906	NZ_GG668576	copC	ZP_03839688.1	130	Copper resistance protein CopC.
PATRIC	*E. coli* 7-233-03_S4_C2	JORW01000046	copB	KEN13242.1	296	Copper resistance protein B.
PATRIC	*P. mirabilis* ATCC 29906	NZ_GG668576	cutC	ZP_03839779.1	250	Copper homeostasis protein CutC (Cytoplasmic copper homeostasis protein CutC).
RefSeq	*P. mirabilis* BB2000	CP004022	cop A	AGS60771.1	904	Copper exporting ATPase.
PATRIC	*P. mirabilis* ATCC 29906	NZ_GG668576	cop A	ZP_03840922.1	949	Lead, cadmium, zinc and mercury transporting ATPase (EC 3.6.3.3) (EC 3.6.3.5); Copper-translocating P-type ATPase (EC 3.6.3.4).
RefSeq	*P. mirabilis* strain ATCC 7002	JOVJ01000009	kdpB	KGA89427.1	685	Copper exporting ATPase (potassium-transporting ATPase subunit B).

RefSeq	*P. mirabilis*	WP_012368272.1, WP_020946123.1	copA-CopZ-HMA	WP_012368272 WP_020946123	984	Copper exporting ATPase (Heavy-metal-associated domain (HMA)).
RefSeq	*P. mirabilis* strain ATCC 7002	JOVJ01000005	cueR	KGA91278.1	135	Copper -responsive transcriptional regulator (HTH_MerR-SF Superfamily).
PATRIC	*P. mirabilis* BB2000 *P. mirabilis* strain 1310_PMIR	CP004022 JVUH01000152 JVUH01001396	cutF	ZP_03841587.1 PGF_00241126* PGF_00241126*	225 154 78	Copper homeostasis protein CutF precursor / Lipoprotein NlpE involeved in surface adhesion.
PATRIC RefSeq	*P. mirabilis* BB2000	CP004022	terB terA terC terD terE terZ	AGS60978.1 AGS60979.1 AGS60977.1 AGS60976.1 AGS60975.1 AGS60980.1	151 382 341 192 191 194	*P. mirabilis* tellurite resistance loci.
PATRIC RefSeq	*Mycobacterium sp.*	YP_001705575.1 CP002992	ctpC	AEN01737.1	718	Probable cation-transporting ATPase G (ATPase-IB2_Cd).
PATRIC	*P. mirabilis* ATCC 29906	NZ_GG668579	yntB	ZP_03841770.1	325	Nickel transport system permease protein nikB2 (TC 3.A.1.5.3).
PATRIC	*P. mirabilis* ATCC 29906	NZ_GG668579	yntA	ZP_03841771.1	527	Nickel ABC transporter, periplasmic nickel-binding protein nikA2 (TC 3.A.1.5.3).
PATRIC	*P. mirabilis* ATCC 29906	NZ_GG668583	NA	ZP_03839446.1	289	Nickel transport system permease protein NikC (TC 3.A.1.5.3).
PATRIC	*P. mirabilis* ATCC 29906	NZ_GG668583	NA	ZP_03839447.1	269	Nickel transport ATP-binding protein NikD (TC 3.A.1.5.3).
PATRIC	*P. mirabilis* ATCC 29906	NZ_GG668579	yntD	ZP_03841768.1	267	Nickel transport ATP-binding protein nikD2 (TC 3.A.1.5.3).
PATRIC	*P. mirabilis* ATCC 29906	NZ_GG668579	yntE	ZP_03841767.1	203	Nickel transport ATP-binding protein nikE2 (TC 3.A.1.5.3).
PATRIC	*P. mirabilis* ATCC 29906	NZ_GG668579	yntC	ZP_03841769.1	270	Nickel transport system permease protein nikC2 (TC 3.A.1.5.3).
PATRIC	*P. mirabilis* BB2000	CP004022	hybF	AGS58541.1	113	[NiFe] hydrogenase nickel incorporation protein HypA.
PATRIC	*P. mirabilis* ATCC 29906	NZ_GG668578	hybB	ZP_03842517.1	282	[NiFe] hydrogenase nickel incorporation-associated protein HypB.
RefSeq	*C. crescentus* OR37	APMP01000019	NA	ENZ81282.1	723	Copper/silver/heavy metal-translocating P-type ATPase, Cd/Co/Hg/Pb/Zn-transporting.
RefSeq	*Armatimonadetes* bacterium OLB18 *C. gilvus*	JZQX01000123 WP_013884717.1	arsM	KXK16912.1	283	Arsenite S-adenosylmethyltransferase (Methyltransferase type 11).
RefSeq	*R. palustris* TIE-1	NC_011004	NA	YP_001990857.1	973	Heavy metal translocating P-type ATPase (ATPase-IB1_Cu).
RefSeq	*M. ulcerans* str. Harvey	EUA92940.1,	CuRO_2_CopA_like1	EUA92940.1	552	Multicopper oxidase family protein.
RefSeq	*B. mallei* NCTC 10229	NC_008835	oprB	YP_001024205.1	553	Copper/silver efflux system outer membrane protein CusC (outer membrane efflux protein OprB).
RefSeq	*B. pseudomallei* 576	NZ_ACCE01000001	oprM	ZP_03450560.1	558	Copper/silver efflux system outer membrane protein CusC (outer membrane efflux protein OprM).

PATRIC RefSeq	*Achromobacter sp.* strain 2789STDY5608636 *B. pseudomallei* 1710b	CYTV01000008 ABA52627.1	cusC_1	ABA52627	515	Copper/silver efflux system outer membrane protein CusC (RND efflux system outer membrane lipoprotein).
RefSeq	*Achromobacter sp.* strain 2789STDY5608623	CYSZ01000001	NA	CUI29018.1	98	Outer membrane component of tripartite multidrug resistance system (CusC).
RefSeq	R. opacus	WP_012687282.1 , BAH48260.1	merB	WP_012687282	334	Alkylmercury lyase (MerB).
PATRIC RefSeq	*B. ubonensis* strain MSMB2185WGS	Q44585.1 LPIU01000068	NA	Q44585 PGF_01102114*	379 377	Nickel-cobalt-cadmium resistance protein NccB.
PATRIC	*P. mirabilis* BB2000	CP004022	zntA	AGS58561.1	798	Lead, cadmium, zinc and mercury transporting ATPase (EC 3.6.3.3) (EC 3.6.3.5); Copper-translocating P-type ATPase (EC 3.6.3.4)
PATRIC	*P. mirabilis* BB2000	CP004022	copA	AGS60771.1	949	Lead, cadmium, zinc and mercury transporting ATPase (EC 3.6.3.3) (EC 3.6.3.5); Copper-translocating P-type ATPase (EC 3.6.3.4).
PATRIC	*P. mirabilis* BB2000	CP004022	copA	AGS60770.1	54	Lead, cadmium, zinc and mercury transporting ATPase (EC 3.6.3.3) (EC 3.6.3.5); Copper-translocating P-type ATPase (EC 3.6.3.4).

Discussion:

Proteus mirabilis SCDR1 isolate was isolated from a Diabetic ulcer patient visiting the Diabetic foot unit unit in the University Diabetes Center at King Saud University in the University Diabetes Center at King Saud University. Our SCDR1 isolate was observed as mixed culture along with *S. aureus* isolate while testing our produced silver Nanoparticles against several pathogenic *S. aureus* isolates (Saeb et al. 2014). Whereas other tested Gram positive and negative bacteria showed great sensitivity against silver Nanoparticles, *P. mirabilis* SCDR1 isolate exhibited extreme resistance. *P. mirabilis* SCDR1 isolate is multi-drug resistant bacteria (MDR), since, our isolate was non-susceptible to at least one agent in at least three antimicrobial categories (Magiorakos et al. 2012). Our isolate was against ansamycins, glycopeptides, fucidanes, cyclic peptides, nitroimidazoles, macrolides, lincosamides, folate pathway inhibitors and

aminocoumarin antimicrobial categories. Moreover, our isolate exhibited the intrinsic resistant against tetracyclines and polymyxins specific to *P. mirabilis* species (Chen et al. 2015). However, fortunately, our isolates is sensitive against several operational antimicrobial categories such as penicillins with b-lactamase inhibitors, extended-spectrum cephalosporins, carbapenems, aminoglycosides, fluoroquinolones and phosphonic acids. In addition, our *P. mirabilis* SCDR1 isolate showed high resistance against colloidal and composite Nanosilver and metallic silver when compared to other tested Gram positive and negative bacterial species both qualitatively and quantitatively. To our knowledge, this is the first reported case of bacterial spontaneous resistance to colloidal and composite Nano-Silver. *P. mirabilis SCDR1* demonstrated resistance against colloidal Nanosilver assessed either by disk diffusion or by minimal inhibitory concentration methods. While, all used concentrations of colloidal Nanosilver have shown strong effects on all tested microorganisms (Table 1), no effect on the bacterial growth of *P. mirabilis SCDR1* even at the highest used concentration (200 ppm). Similarly, *P. mirabilis SCDR1* were able to resist ten folds (500 ppm) higher than *K. pneumoniae* (50 ppm), five folds higher than *P. aeruginosa* and *E. coli* (100 ppm) and two and a half folds (200 ppm) higher than *S. aureus* and *E. cloacae* (Table 2). Moreover, while both laboratories prepared and commercially available silver and Nanosilver composite showed a clear effect against both *S. aureus* and *P. aeruginosa* the most common pathogens of diabetic foot ulcer, not effect was observed against *P. mirabilis SCDR1* (Table 3). Although chitosan nanosilver composites have documented combined effect against both Gram positive and negative pathogens (Latif et al. 2015) no effect was observed against *P. mirabilis SCDR1*.

P. mirabilis SCDR1 genome analysis showed that our isolate contains a large number of genes (245) responsible for xenobiotics biodegradation and metabolism (**supplementary table 2**). These includes Atrazine, Naphthalene and Trinitrotoluene degradation. In addition, we detected the presence genes encoding for the members Chitosanase family GH3 of N, N'-diacetylchitobiose-specific 6-phospho-beta-glucosidase (EC 3.2.1.86), Beta N-acetyl-glucosaminidase (nagZ, beta-hexosaminidase) (EC 3.2.1.52), and Glucan endo-1, 4-beta-glucosidase (EC 3.2.1.-) in *P. mirabilis* SCDR1 suggests that it can hydrolyze

chitosan to glucosamine (Wieczorek et al. 2014; Gupta et al. 2010, 2011). This justifies the lack of antimicrobial effect of chitosan against *P. mirabilis SCDR1*.

Similarly, *P. mirabilis* SCDR1 showed resistance against all the tested commercially available silver and Nanosilver containing wound dressing bandages. These silver containing commercially available bandages (wound dressing material) use different manufacturing technology and constituents. For example, Silvercel wound dressing contains high G calcium alginate in addition to 28% Silver-coated fibers (dressing contains 111mg silver/100cm^2). The silver-coated fibers encompass elemental silver, which is converted to silver oxide upon contact with oxygen. Silver oxide dissolves in fluid and releases ionic silver (Ag^+) that have antimicrobial action (Cutting et al. 2007). Clinical studies showed that Silvercel wound dressing is effective against many common wound pathogens, including methicillin-resistant Staphylococcus aureus (MRSA), methicillin -resistant Staphylococcus epidermidis (MRSE) and vancomycin-resistant Enterococcus (VRE). In addition, these studies showed that Silvercel wound dressing prevented and disrupted the formation of bacterial biofilms (McInroy et al. 2010; Stephens et al. 2010). However, this was not the case with our *P. mirabilis* SCDR1 isolate.

Pathogenomics analysis showed that *P. mirabilis* SCDR1 isolate is a potential virulent pathogen that despite its original isolation site, wound, it can establish kidney infection and its associated complications (**Supplementary tables 3 and 4**). *P. mirabilis* SCDR1 showed that it possesses the characteristic bull's eye pattern swarming behavior. Presenting swarmer cells form is associated with the increase of expression of virulence genes (Allison et al. 1992). Swarming is important to *P. mirabilis* uropathogenesis. When this microorganism presents swarmer cells form, the expression of virulence is increased (Allison et al. 1992). It was shown that swarming bacteria that move in multicellular groups exhibit adaptive resistance to multiple antibiotics (Butler et al. 2010). Moreover, migrating swarm cells display an increased resistance many of antimicrobial agents. For example, swarm cells of *P. aeruginosa* were able to migrate very close to the disc containing arsenite, indicating resistance to this heavy metal (Lai et al. 2009). It was suggested that high densities promote bacterial survival, the ability to move, as well as the speed of movement, confers

an added advantage, making swarming an effective strategy for prevailing against antimicrobials including heavy metals (Lai et al. 2009; Butler et al. 2010). Altruism or self-sacrifice is a suggested phenomenon associated with swarming that involves risk of wiping out some individuals upon movement of bacteria to a different location allowing the remaining individuals to continue their quest (Butler et al. 2010; Gadagkar 1997). Thus maintaining high cell density, though the observed quorum sensing ability (**supplementary table 4**), circulating within the multilayered colony to minimize exposure to the heavy metal, and the death of individuals that are directly exposed could be the key to the observed Nanosilver resistance.

P. mirabilis SCDR1 isolate exhibited the ability of biofilm formation and also our pathogenomics analysis showed that it contains genes responsible for it such as glpC gene coding for anaerobic glycerol-3-phosphate dehydrogenase subunit C (EC 1.1.5.3), pmrI gene coding for UDP-glucuronic acid decarboxylase and baaS gene coding for biofilm formation regulatory protein BssS. Uropathogens use different mechanisms including biofilm formation for survival in response to stresses in the bladder such as starvation and immune responses (Justice et al. 2008; Horvath et al. 2011). Also, biofilm formation can reduce the metal toxic effect by trapping it outside the cells. It was found that in the relative bacteria *Proteus vulgaris* XC 2 the biofilm cells of showed considerably greater resistance to Chloromycetin compared to planktonic cells (free-floating counterparts) (Wu et al. 2015). In addition, it was found that biofilm formation and exopolysaccharide are very important for the heavy metal resistance in *Pseudomonas* sp. and that biofilm lacking mutant was less tolerant to heavy metals (Chien et al. 2013). Furthermore, it was found that both extracellular polysaccharides and biofilm formation is a resistance mechanism against to toxic metals in *Sinorhizobium meliloti*, the nitrogen-fixing bacterium (Nocelli et al. 2016). Thus, we suggest that the ability of *P. mirabilis* SCDR1 to form biofilm may also assist in the observed Nanosilver resistance.

In addition, *P. mirabilis* SCDR1 contains several genes and proteins that also facilitate metal resistance including silver and Nanosilver (**table 6**). We observed the presence of gene determinants of Copper/silver efflux system, oprB encoding for Copper/silver efflux system outer membrane protein CusC (outer

membrane efflux protein OprB), oprM encoding for Copper/silver efflux system outer membrane protein CusC (outer membrane efflux protein OprM), cusC_1 encoding for Copper/silver efflux system outer membrane protein CusC (RND efflux system outer membrane lipoprotein), cpxA encoding for Copper sensory histidine kinase and outer membrane component of tripartite multidrug resistance system (CusC). Indicating the presence of endogenous silver and copper resistance mechanism in *P. mirabilis* SCDR1. Similar endogenous silver and copper resistance mechanism has been described in *E. coli* has been associated with loss of porins from the outer membrane and up-regulation of the native Cus efflux mechanism that is capable of transporting silver out of the cell (Li et al. 1997; Lok et al. 2008). Thus we suggest a comprehensive study for this endogenous silver resistance mechanism within *Proteus mirabilis* species.

Furthermore, we observed the presence of enzymes involved in heavy metal resistance such as Glutathione S-transferase (EC 2.5.1.18) (gst1, gst, Delta and Uncharacterized) in *P. mirabilis* SCDR1 genome. Glutathione S-transferases (GSTs) are a family of multifunctional proteins playing important roles in detoxification of harmful physiological and xenobiotic compounds in organisms (Zhang et al. 2013). Moreover, it was found that a Glutathione S-transferase is involved in copper, cadmium, lead and mercury resistance (Nair and Choi 2011). Furthermore, it was found that GST genes are differentially expressed in defense against oxidative stress caused by Cd and Nanosilver exposure (Nair and Choi 2011). Thus we can propose a role of Glutathione S-transferases of *P. mirabilis* SCDR1 in the observed Nanosilver resistance. Moreover, we observed the presence of a complete tellurite resistance operon (terB, terA, terC, terD, terE, terZ) that was suggested to contribute to virulence or fitness and protection from other forms of oxidative stress or agents causing membrane damage, such as silver and Nanosilver, in *P. mirabilis* (Toptchieva et al. 2003).

Several other heavy metal resistance genes and proteins were observed in the *P. mirabilis* SCDR1 genome. Such as, arsM encoding for arsenite S-adenosylmethyltransferase (Methyltransferase type 11) that play important role in prokaryotic resistance and detoxification mechanism to arsenite (Qin et al. 2009, 2006)

and merB encoding for alkylmercury lyase that cleaves the carbon-mercury bond of organomercurials such as phenylmercuric acetate (Marchler-Bauer et al. 2015).

In addition, we observed the presence of several multidrug resistance efflux systems and complexes such as MdtABC-TolC, which is a multidrug efflux system in Gram-negative bacteria, including *E. coli* and *Salmonella* that confer resistance against β-lactams, novobiocin and deoxycholate (Nishino et al. 2007). It is noteworthy to mention that MdtABC-TolC and AcrD paly role in metal resistance (copper and zinc) along with their BaeSR regulatory system (Franke et al. 2003) that also was found in our *P. mirabilis* SCDR1 genome [**table 5**] thus also may play additional role in silver resistance. The MdtABC and AcrD systems may be related to bacterial metal homeostasis by transporting metals directly. This is to some extent similar to the copper and silver resistance mechanism by cation efflux of the CusABC system belonging to the RND protein superfamily (Franke et al. 2003; Outten et al. 2001). In addition, our isolate contains MacAB-TolC efflux pump which is an ABC efflux pump complex expressed in *E. coli* and *Salmonella enterica* and confers resistance to macrolides, including erythromycin (Nishino et al. 2006). Furthermore, we detected that presence of AcrAB-TolC efflux pump which is a tripartite RND efflux system that confers resistance to tetracycline, chloramphenicol, ampicillin, nalidixic acid, and rifampin in Gram-negative bacteria (Tikhonova et al. 2011). Moreover, EmrAB-TolC efflux system that confer resistance to nalidixic acid and thiolactomycin was also observed (Lomovskaya et al. 1995). In addition, AcrEF-TolC, which is a tripartite multidrug efflux system similar to AcrAB-TolC, was found in Gram-negative bacteria (Zheng et al. 2009). Finally, Multidrug and toxic compound extrusion (MATE) system was observed in *P. mirabilis*-SCDR1 genome. It is responsible for Directed pumping of antibiotic out of a cell and thus of resistance. It utilizes the cationic gradient across the membrane as an energy source. Generally, the resistance gene search, resistome analysis, was in great agreement with the antibiotic sensitivity testing with very few exceptions. For example, several chloramphenicol resistance genes and proteins such as cpxR, cpxA, cat and AcrAB-TolC efflux pump were observed, though our *P. mirabilis* SCDR1 isolate was

chloramphenicol sensitive. Yet genomic resistome analysis proofed to be a successful way of testing drug resistance and even discovering potential drug resistance genes in a given bacterium.

It is also worth mentioning that some cases we observed *P. mirabilis* SCDR1 adaptive resistance against and/secondary waves of swarming some antibiotics that initially scored as sensitive. These antibiotic belongs to the aminoglycosides (Spectinomycin and Streptomycin), cephalosporins (Ceftriaxone, Cefoxitin, Cephalothin, Cefotaxime, Cefaclor and Cefepime) and β-lactams (Aztreonam and Meropenem). Similar observations were also detected with *B. subtilis*, *B. thailandensis*, *E. coli* and (Lai et al. 2009) *Salmonella enterica* serovar Typhimurium (Tikhonova et al. 2011). Adaptation, rather than mutation, to increasing levels of antibiotics was suggested to justify the observed swarm waves.

The increasing antimicrobial nanosilver usage could prompt a silver resistance problem in Gram-negative pathogens, particularly since silver resistance is already known to exist in several such species (Li et al. 1997; Andersson 2003). Both exogenous (horizontally acquired Sil system) endogenous (mutational Cus system) resistance to silver has been reported in Gram-negative bacteria (Li et al. 1997; McHugh et al. 1975). Similarly, in our case we observed the presence of resistance operon with high similarity with the *cus* operon that is, in turn, is chromosomally encoded system because of the lack of any plasmid in *P. mirabilis* SCDR1. However, both endogenous and exogenous silver resistance systems, in Gram-negative bacteria, remain incompletely understood (Randall et al. 2015).

The occurrence of induced nanosilver resistance (in vitro) in *Bacillus sp.* (Gunawan et al. 2013), spontaneous resistance (in our case) and the frequent uses and misuses of nanosilver-containing medical products should suggest adopting an enhanced surveillance systems for nanosilver-resistant isolates in the medical setups. In addition, greater control over utilizing nanosilver-containing products should also be adapted in order to maintain nanosilver as valuable alternative approach for fighting multidrug resistant pathogens.

Conclusion:

In the present study, we introduced the *P. mirabilis SCDR1* isolate that was collected from a Diabetic ulcer patient. *P. mirabilis SCDR1* showed high levels of resistance against Nano-silver colloids, Nano-silver chitosan composite and the commercially available Nano-silver and silver bandages. Our isolate contains all the required pathogenicity and virulence factors to establish a successful infection. *P. mirabilis SCDR1* contains several physical and biochemical mechanisms for antibiotics and silver/nanosilver resistance, which are biofilm formation, swarming mobility, efflux systems, and enzymatic detoxification**.**

Acknowledgement:

The authors want to thank the members of the Diabetic foot unit in the University Diabetes Center at King Saud University for their help in collecting the bacteria samples. Furthermore, we want to thanks the members of the nanotechnology department in SCDR for providing the chitosan nanosilver composites. In addition we want to acknowledge that NGS experiments and analysis were supported by the Saudi Human Genome Program (SHGP) at KACST and KFSHRC. Moreover, we want to thank Dr. Rebecca Wattam, form the Biocomplexity Institute at Virginia Polytechnic Institute and State University, for her great assistance during data analysis using PATRIC services and tools.

References

Abouelhoda M, Issa SA, Ghanem M. 2012. Tavaxy: integrating Taverna and Galaxy workflows with cloud computing support. *BMC Bioinformatics* **13**: 77.

Abouelhoda MI, Kurtz S, Ohlebusch E. 2008. CoCoNUT: an efficient system for the comparison and analysis of genomes. *BMC Bioinformatics* **9**: 476.

Allison C, Lai HC, Hughes C. 1992. Co-ordinate expression of virulence genes during swarm-cell differentiation and population migration of Proteus mirabilis. *Mol Microbiol* **6**: 1583–1591.

577 Andersson DI. 2003. Persistence of antibiotic resistant bacteria. *Curr Opin Microbiol* **6**: 452–456.

578 Armbruster CE, Mobley HLT. 2012. Merging mythology and morphology: the multifaceted lifestyle of
579 Proteus mirabilis. *Nat Rev Microbiol* **10**: 743–754.

580 Baldo C, Rocha SPD. 2014. Virulence Factors Of Uropathogenic Proteus Mirabilis - A Mini Review. *Int*
581 *J Technol Enhanc Emerg Eng Res* **3**: 24–27.

582 Bronze MS, Cunha BA. 2016. Diabetic Foot Infections: Practice Essentials, Background,
583 Pathophysiology. http://emedicine.medscape.com/article/237378-overview (Accessed November
584 3, 2016).

585 Butler MT, Wang Q, Harshey RM. 2010. Cell density and mobility protect swarming bacteria against
586 antibiotics. *Proc Natl Acad Sci U S A* **107**: 3776–3781.

587 Caporaso JG, Kuczynski J, Stombaugh J, Bittinger K, Bushman FD, Costello EK, Fierer N, Peña AG,
588 Goodrich JK, Gordon JI, et al. 2010. QIIME allows analysis of high-throughput community
589 sequencing data. *Nat Methods* **7**: 335–336.

590 Chen L, Al Laham N, Chavda KD, Mediavilla JR, Jacobs MR, Bonomo RA, Kreiswirth BN. 2015. First
591 report of an OXA-48-producing multidrug-resistant Proteus mirabilis strain from Gaza, Palestine.
592 *Antimicrob Agents Chemother* **59**: 4305–4307.

593 Chen X, Schluesener HJ. 2008. Nanosilver: a nanoproduct in medical application. *Toxicol Lett* **176**: 1–12.

594 Chien C-C, Lin B-C, Wu C-H. 2013. Biofilm formation and heavy metal resistance by an environmental
595 Pseudomonas sp. *Biochem Eng J* **78**: 132–137.

596 Cosentino S, Voldby Larsen M, Møller Aarestrup F, Lund O. 2013. PathogenFinder--distinguishing
597 friend from foe using bacterial whole genome sequence data. *PloS One* **8**: e77302.

598 Cutting K, White R, Edmonds M. 2007. The safety and efficacy of dressings with silver - addressing
599 clinical concerns. *Int Wound J* **4**: 177–184.

600 Darling ACE, Mau B, Blattner FR, Perna NT. 2004. Mauve: multiple alignment of conserved genomic
601 sequence with rearrangements. *Genome Res* **14**: 1394–1403.

602 Franci G, Falanga A, Galdiero S, Palomba L, Rai M, Morelli G, Galdiero M. 2015. Silver nanoparticles as
603 potential antibacterial agents. *Mol Basel Switz* **20**: 8856–8874.

604 Franke S, Grass G, Rensing C, Nies DH. 2003. Molecular analysis of the copper-transporting efflux
605 system CusCFBA of Escherichia coli. *J Bacteriol* **185**: 3804–3812.

606 Gadagkar R. 1997. *SURVIVAL STRATEGIES: COOPERATION AND CONFLICT IN ANIMAL*
607 *SOCIETIES.* Harvard University Press, Cambridge, Massachusetts
608 https://www.researchgate.net/publication/276238210_Gadagkar_R_1997_SURVIVAL_STRATE
609 GIES_COOPERATION_AND_CONFLICT_IN_ANIMAL_SOCIETIES_Harvard_University_P
610 ress_Cambridge_Massachusetts_x_196_pp_ISBN_0-674-17055-5_price_hardcover_2200
611 (Accessed November 3, 2016).

612 Gonzalez G, Bronze MS. 2016. Proteus Infections: Background, Pathophysiology, Epidemiology.
613 http://emedicine.medscape.com/article/226434-overview (Accessed November 3, 2016).

614 Gunawan C, Teoh WY, Marquis CP, Amal R. 2013. Induced adaptation of Bacillus sp. to antimicrobial
615 nanosilver. *Small Weinh Bergstr Ger* **9**: 3554–3560.

616 Gupta V, Prasanna R, Natarajan C, Srivastava AK, Sharma J. 2010. Identification, characterization, and
617 regulation of a novel antifungal chitosanase gene (cho) in Anabaena spp. *Appl Environ Microbiol*
618 **76**: 2769–2777.

619 Gupta V, Prasanna R, Srivastava AK, Sharma J. 2011. Purification and characterization of a novel
620 antifungal endo-type chitosanase from Anabaena fertilissima. *Ann Microbiol* **62**: 1089–1098.

621 Habibi M, Asadi Karam MR, Bouzari S. 2015. In silico design of fusion protein of FimH from
622 uropathogenic Escherichia coli and MrpH from Proteus mirabilis against urinary tract infections.
623 *Adv Biomed Res* **4**: 217.

624 Hawser SP, Badal RE, Bouchillon SK, Hoban DJ, Hackel MA, Biedenbach DJ, Goff DA. 2014.
625 Susceptibility of gram-negative aerobic bacilli from intra-abdominal pathogens to antimicrobial
626 agents collected in the United States during 2011. *J Infect* **68**: 71–76.

627 Hendry AT, Stewart IO. 1979. Silver-resistant Enterobacteriaceae from hospital patients. *Can J Microbiol*
628 **25**: 915–921.

629 Holla G, Yeluri R, Munshi AK. 2012. Evaluation of minimum inhibitory and minimum bactericidal
630 concentration of nano-silver base inorganic anti-microbial agent (Novaron(®)) against
631 streptococcus mutans. *Contemp Clin Dent* **3**: 288–293.

632 Horner CS, Abberley N, Denton M, Wilcox MH. 2014. Surveillance of antibiotic susceptibility of
633 Enterobacteriaceae isolated from urine samples collected from community patients in a large
634 metropolitan area, 2010-2012. *Epidemiol Infect* **142**: 399–403.

635 Horvath DJ, Li B, Casper T, Partida-Sanchez S, Hunstad DA, Hultgren SJ, Justice SS. 2011.
636 Morphological plasticity promotes resistance to phagocyte killing of uropathogenic Escherichia
637 coli. *Microbes Infect* **13**: 426–437.

638 Jacobsen SM, Stickler DJ, Mobley HLT, Shirtliff ME. 2008. Complicated catheter-associated urinary
639 tract infections due to Escherichia coli and Proteus mirabilis. *Clin Microbiol Rev* **21**: 26–59.

640 Jansen AM, Lockatell CV, Johnson DE, Mobley HLT. 2003. Visualization of Proteus mirabilis
641 morphotypes in the urinary tract: the elongated swarmer cell is rarely observed in ascending
642 urinary tract infection. *Infect Immun* **71**: 3607–3613.

643 Justice SS, Hunstad DA, Cegelski L, Hultgren SJ. 2008. Morphological plasticity as a bacterial survival
644 strategy. *Nat Rev Microbiol* **6**: 162–168.

645 Lai S, Tremblay J, Déziel E. 2009. Swarming motility: a multicellular behaviour conferring antimicrobial
646 resistance. *Environ Microbiol* **11**: 126–136.

647 Latif U, Al-Rubeaan K, Saeb ATM. 2015. A Review on Antimicrobial Chitosan-Silver Nanocomposites:
648 A Roadmap Toward Pathogen Targeted Synthesis. *Int J Polym Mater Polym Biomater* **64**: 448–
649 458.

650 Li XZ, Nikaido H, Williams KE. 1997. Silver-resistant mutants of Escherichia coli display active efflux
651 of Ag+ and are deficient in porins. *J Bacteriol* **179**: 6127–6132.

652 Liu B, Pop M. 2009. ARDB--Antibiotic Resistance Genes Database. *Nucleic Acids Res* **37**: D443-447.

653 Lok C-N, Ho C-M, Chen R, Tam PK-H, Chiu J-F, Che C-M. 2008. Proteomic identification of the Cus
654 system as a major determinant of constitutive Escherichia coli silver resistance of chromosomal
655 origin. *J Proteome Res* **7**: 2351–2356.

656 Lomovskaya O, Lewis K, Matin A. 1995. EmrR is a negative regulator of the Escherichia coli multidrug
657 resistance pump EmrAB. *J Bacteriol* **177**: 2328–2334.

658 Lullove EJ, Bernstein B. 2015. Use of SilvrSTAT® in lower extremity wounds: a two center case series
659 « Journal of Diabetic Foot Complications. **7**: 13–16.

660 Magiorakos A-P, Srinivasan A, Carey RB, Carmeli Y, Falagas ME, Giske CG, Harbarth S, Hindler JF,
661 Kahlmeter G, Olsson-Liljequist B, et al. 2012. Multidrug-resistant, extensively drug-resistant and
662 pandrug-resistant bacteria: an international expert proposal for interim standard definitions for
663 acquired resistance. *Clin Microbiol Infect Off Publ Eur Soc Clin Microbiol Infect Dis* **18**: 268–
664 281.

665 Marchler-Bauer A, Derbyshire MK, Gonzales NR, Lu S, Chitsaz F, Geer LY, Geer RC, He J, Gwadz M,
666 Hurwitz DI, et al. 2015. CDD: NCBI's conserved domain database. *Nucleic Acids Res* **43**: D222-
667 226.

668 Mathur S, Sabbuba NA, Suller MTE, Stickler DJ, Feneley RCL. 2005. Genotyping of urinary and fecal
669 Proteus mirabilis isolates from individuals with long-term urinary catheters. *Eur J Clin Microbiol*
670 *Infect Dis Off Publ Eur Soc Clin Microbiol* **24**: 643–644.

671 Matuschek E, Brown DFJ, Kahlmeter G. 2014. Development of the EUCAST disk diffusion antimicrobial
672 susceptibility testing method and its implementation in routine microbiology laboratories. *Clin*
673 *Microbiol Infect Off Publ Eur Soc Clin Microbiol Infect Dis* **20**: O255-266.

674 McArthur AG, Waglechner N, Nizam F, Yan A, Azad MA, Baylay AJ, Bhullar K, Canova MJ, De
675 Pascale G, Ejim L, et al. 2013. The comprehensive antibiotic resistance database. *Antimicrob*
676 *Agents Chemother* **57**: 3348–3357.

677 McArthur AG, Wright GD. 2015. Bioinformatics of antimicrobial resistance in the age of molecular
678 epidemiology. *Curr Opin Microbiol* **27**: 45–50.

679 McHugh GL, Moellering RC, Hopkins CC, Swartz MN. 1975. Salmonella typhimurium resistant to silver
680 nitrate, chloramphenicol, and ampicillin. *Lancet Lond Engl* **1**: 235–240.

McInroy L, Cullen B, Clark R. 2010. Are silver-containing dressings effective against bacteria in biofilms? www.systagenix.it/cms/uploads/McInroy_biofilms_SAWC_2010.pdf.

Miró E, Agüero J, Larrosa MN, Fernández A, Conejo MC, Bou G, González-López JJ, Lara N, Martínez-Martínez L, Oliver A, et al. 2013. Prevalence and molecular epidemiology of acquired AmpC β-lactamases and carbapenemases in Enterobacteriaceae isolates from 35 hospitals in Spain. *Eur J Clin Microbiol Infect Dis Off Publ Eur Soc Clin Microbiol* **32**: 253–259.

Nair PMG, Choi J. 2011. Identification, characterization and expression profiles of Chironomus riparius glutathione S-transferase (GST) genes in response to cadmium and silver nanoparticles exposure. *Aquat Toxicol Amst Neth* **101**: 550–560.

Nishino K, Latifi T, Groisman EA. 2006. Virulence and drug resistance roles of multidrug efflux systems of Salmonella enterica serovar Typhimurium. *Mol Microbiol* **59**: 126–141.

Nishino K, Nikaido E, Yamaguchi A. 2007. Regulation of multidrug efflux systems involved in multidrug and metal resistance of Salmonella enterica serovar Typhimurium. *J Bacteriol* **189**: 9066–9075.

Nocelli N, Bogino PC, Banchio E, Giordano W. 2016. Roles of Extracellular Polysaccharides and Biofilm Formation in Heavy Metal Resistance of Rhizobia. *Materials* **9**: 418.

Outten FW, Huffman DL, Hale JA, O'Halloran TV. 2001. The independent cue and cus systems confer copper tolerance during aerobic and anaerobic growth in Escherichia coli. *J Biol Chem* **276**: 30670–30677.

Oyanedel-Craver VA, Smith JA. 2008. Sustainable colloidal-silver-impregnated ceramic filter for point-of-use water treatment. *Environ Sci Technol* **42**: 927–933.

Pal C, Bengtsson-Palme J, Rensing C, Kristiansson E, Larsson DGJ. 2014. BacMet: antibacterial biocide and metal resistance genes database. *Nucleic Acids Res* **42**: D737-743.

703 Prabhu S, Poulose EK. 2012. Silver nanoparticles: mechanism of antimicrobial action, synthesis, medical
704 applications, and toxicity effects. *Int Nano Lett* **2**: 32.

705 Qin J, Lehr CR, Yuan C, Le XC, McDermott TR, Rosen BP. 2009. Biotransformation of arsenic by a
706 Yellowstone thermoacidophilic eukaryotic alga. *Proc Natl Acad Sci U S A* **106**: 5213–5217.

707 Qin J, Rosen BP, Zhang Y, Wang G, Franke S, Rensing C. 2006. Arsenic detoxification and evolution of
708 trimethylarsine gas by a microbial arsenite S-adenosylmethionine methyltransferase. *Proc Natl*
709 *Acad Sci U S A* **103**: 2075–2080.

710 Randall CP, Gupta A, Jackson N, Busse D, O'Neill AJ. 2015. Silver resistance in Gram-negative bacteria:
711 a dissection of endogenous and exogenous mechanisms. *J Antimicrob Chemother* **70**: 1037–1046.

712 Saeb ATM, Alshammari AS, Al-Brahim H, Al-Rubeaan KA. 2014. Production of silver nanoparticles
713 with strong and stable antimicrobial activity against highly pathogenic and multidrug resistant
714 bacteria. *ScientificWorldJournal* **2014**: 704708.

715 Segata N, Waldron L, Ballarini A, Narasimhan V, Jousson O, Huttenhower C. 2012. Metagenomic
716 microbial community profiling using unique clade-specific marker genes. *Nat Methods* **9**: 811–
717 814.

718 Stephens S, Clark R, Del Bono M, Snyder R. 2010. Designing In Vitro, In Vivo and Clinical Evaluations
719 to meet the Needs of the Patient and Clinician: Dressing Wound Adherence.

720 Tamura K, Nei M. 1993. Estimation of the number of nucleotide substitutions in the control region of
721 mitochondrial DNA in humans and chimpanzees. *Mol Biol Evol* **10**: 512–526.

722 Tamura K, Stecher G, Peterson D, Filipski A, Kumar S. 2013. MEGA6: Molecular Evolutionary Genetics
723 Analysis version 6.0. *Mol Biol Evol* **30**: 2725–2729.

724 Tikhonova EB, Yamada Y, Zgurskaya HI. 2011. Sequential mechanism of assembly of multidrug efflux
725 pump AcrAB-TolC. *Chem Biol* **18**: 454–463.

726 Toptchieva A, Sisson G, Bryden LJ, Taylor DE, Hoffman PS. 2003. An inducible tellurite-resistance
727 operon in Proteus mirabilis. *Microbiol Read Engl* **149**: 1285–1295.

728 Velázquez-Velázquez JL, Santos-Flores A, Araujo-Meléndez J, Sánchez-Sánchez R, Velasquillo C,
729 González C, Martínez-Castañon G, Martinez-Gutierrez F. 2015. Anti-biofilm and cytotoxicity
730 activity of impregnated dressings with silver nanoparticles. *Mater Sci Eng C Mater Biol Appl* **49**:
731 604–611.

732 VFDB: Virulence Factors Database. 2003. *Virulance Factors Pathog Bact*. http://www.mgc.ac.cn/VFs/
733 (Accessed November 3, 2016).

734 Wattam AR, Abraham D, Dalay O, Disz TL, Driscoll T, Gabbard JL, Gillespie JJ, Gough R, Hix D,
735 Kenyon R, et al. 2014. PATRIC, the bacterial bioinformatics database and analysis resource.
736 *Nucleic Acids Res* **42**: D581-591.

737 Wieczorek AS, Hetz SA, Kolb S. 2014. Microbial responses to chitin and chitosan in oxic and anoxic
738 agricultural soil slurries. *Biogeosciences* **11**: 3339–3352.

739 Wu YL, Liu KS, Yin XT, Fei RM. 2015. GlpC gene is responsible for biofilm formation and defense
740 against phagocytes and imparts tolerance to pH and organic solvents in Proteus vulgaris. *Genet*
741 *Mol Res GMR* **14**: 10619–10629.

742 Yassien M, Khardori N. 2001. Interaction between biofilms formed by Staphylococcus epidermidis and
743 quinolones. *Diagn Microbiol Infect Dis* **40**: 79–89.

744 Zankari E, Hasman H, Cosentino S, Vestergaard M, Rasmussen S, Lund O, Aarestrup FM, Larsen MV.
745 2012. Identification of acquired antimicrobial resistance genes. *J Antimicrob Chemother* **67**:
746 2640–2644.

747 Zhang W, Yin K, Li B, Chen L. 2013. A glutathione S-transferase from Proteus mirabilis involved in
748 heavy metal resistance and its potential application in removal of Hg^{2+}. *J Hazard Mater* **261**:
749 646–652.

750 Zheng J, Cui S, Meng J. 2009. Effect of transcriptional activators RamA and SoxS on expression of
751 multidrug efflux pumps AcrAB and AcrEF in fluoroquinolone-resistant Salmonella
752 Typhimurium. *J Antimicrob Chemother* **63**: 95–102.

753
754
755
756
757
758
759
760
761
762
763
764
765
766
767

768 * **List of abbreviations**

769 **NGS:** Next generation sequencing techniques

770 **16S rRNA:** 16S ribosomal RNA gene

771 **Mb:** Mega base pairs

772 **GC content:** guanine-cytosine content

773 **BLASTn:** Basic Local Alignment Search Tool nucleotide

774 **bp:** Base pair

775 **SCDR:** Strategic center for Diabetes research

776 **KFSHRC:** King Faisal Specialist Hospital and Research Center

777 **PATRIC:** Pathosystems recourse Integration center

778 **DFU:** Diabetic foot ulcer

779 **MDR:** multidrug-resistant

780 **PPM:** part per million

781 **tRNAs:** Transfer ribonucleic acid

782 **AROs:** Antibiotic Resistance Ontology

783 **AMRO:** Antimicrobial Resistance based ontology

784 **RGI:** Resistance Gene Identifier

785 **DDT:** 1, 1, 1-Trichloro-2, 2-bis (4-chlorophenyl) ethane

786 **MRSA:** methicillin-resistant Staphylococcus aureus

787 **MRSE:** methicillin -resistant Staphylococcus epidermidis

788 **VRE:** Vancomycin-resistant Enterococcus

789 **MIC:** Minimum Inhibitory Concentration

790 **RND:** Resistance-Nodulation- Division

791

792

793

Declarations:

*** Ethics approval and consent to participate**

This study was approved by institutional review board in King Saud University, Collage of Medicine Riyadh, Kingdom of Saudi Arabia. The subject was provided written informed consent for participating in this study.

*** Consent to publish**

All other have consented for publication of this manuscript.

* **Availability of data and materials**

Data from our draft genome of *P. mirabilis* SCDR1 isolate was deposited in NCBI-GenBank with an accession number LUFT00000000.

* **Competing interests**

The authors declare that they have no competing interests

*** Funding**

The authors received internal research fund from King Faisal specialist hospital and research center to support the publication.

* **Authors' contributions**

ATMS: Involved in study conception and design, data analysis and interpretation. Involved in drafting the manuscript or revising it critically for important intellectual content. Preparing the final approval of the version to be published.

KA: Involved in study conception and design. Preparing the final approval of the version to be published.

MAH: Involved in study design. Involved in acquisition of data, or analysis and interpretation of data; preparation and involved in drafting the manuscript.

MS: Involved in acquisition of data, or analysis and interpretation of data.

HT: Involved in study conception and design. Involved in drafting the manuscript or revising it critically for important intellectual content. Preparing the final approval of the version to be published.